Document No. [to be completed by the Secretariat] WG-FSA-11/42
Date submitted [to be completed by the Secretariat] 26 September 2011
Language [to be completed by the Secretariat] Original: English
Meeting: WG-FSA Agenda Item No(s): 4.2

Title **Assessment models for Antarctic toothfish (*Dissostichus mawsoni*) in the Ross Sea for the years 1997–98 to 2010–11**

Author(s) S. Mormede[1], A. Dunn[1], & S.M. Hanchet[2]

Address(s) [1]National Institute of Water and Atmospheric Research (NIWA) Ltd
Private Bag 14901, Wellington, New Zealand
[2]National Institute of Water and Atmospheric Research (NIWA) Ltd
P.O. Box 893, Nelson, New Zealand

Name and email address of person submitting paper:
Published or accepted for publication elsewhere? Yes No X
If published or in press, give details:
To be considered for publication in CCAMLR Science*?* Yes No X

Abstract

We provide an update of the Bayesian sex and age structured population stock assessment model for Antarctic toothfish (*Dissostichus mawsoni*) in the Ross Sea region (Subareas 88.1 and SSRUs 88.2A–B), using revised catch, catch-at-age, and tag-recapture data for the 2010–2011 seasons. The 2011 reference model using the selected trips tag data gave a similar, but slightly higher estimate of initial biomass than the 2009 base case. Retrospective analysis suggests that this is partly as a result of the increased number of vessels in selected data set and partly as a result of the 2010 and 2011 observations. Two sensitivity models are presented; the first considers the effect of including possible unaccounted mortality from lost gear, and the second uses tag release and recapture data from all vessel trips.

Overall, model fits to the data were adequate, and, as in previous assessments, the tag-release and recapture data provided the most information on stock size. Monte-Carlo Markov Chain (MCMC) diagnostics suggested little evidence of non-convergence in the key biomass parameters, although there was some evidence of non-convergence in the annual shift parameters for the shelf fishery. MCMC estimates of initial (equilibrium) spawning stock abundance (B_0) for the 2011 reference model were estimated as 73 870 t (95% credible intervals 69 070–78 880), and current (B_{2011}) biomass was estimated as 80.0% B_0 (95% credible intervals 78.6–81.3).The estimated yield, using the CCAMLR decision rules, was 3282 t

Summary of findings as related to nominated agenda items

Agenda Item	*Findings*
4.2	Updated stock assessment for the Ross Sea fishery

1. INTRODUCTION

The exploratory fishery in the Ross Sea region (defined here as Subareas 88.1 and SSRUs 88.2A–B, see Figure 1) was initiated by a New Zealand longline vessel in 1997[1]. Since then, New Zealand vessels and vessels from other countries have returned each summer to fish in this area. Over the last five years, the catch in the toothfish fishery in the Ross Sea region has been between 2200 and 3100 t per annum, and for 2010 and 2011 the catch limit was set at 2850 t (SC-CAMLR-XXVIII 2009).

The catch limits adopted by CCAMLR for 2010 and 2011 were determined from yield estimates from an integrated stock assessment model of Antarctic toothfish in the Ross Sea region (Dunn & Hanchet 2009b). That model assumed a single homogeneous area with three geographically defined fisheries (shelf, slope and north, see later). Data included were based on total catch (C2 data); catch-at-age frequencies using the tree regression post-stratification (Phillips et al. 2005) and tag-release and recapture data up to 2009 (Dunn et al. 2009a).

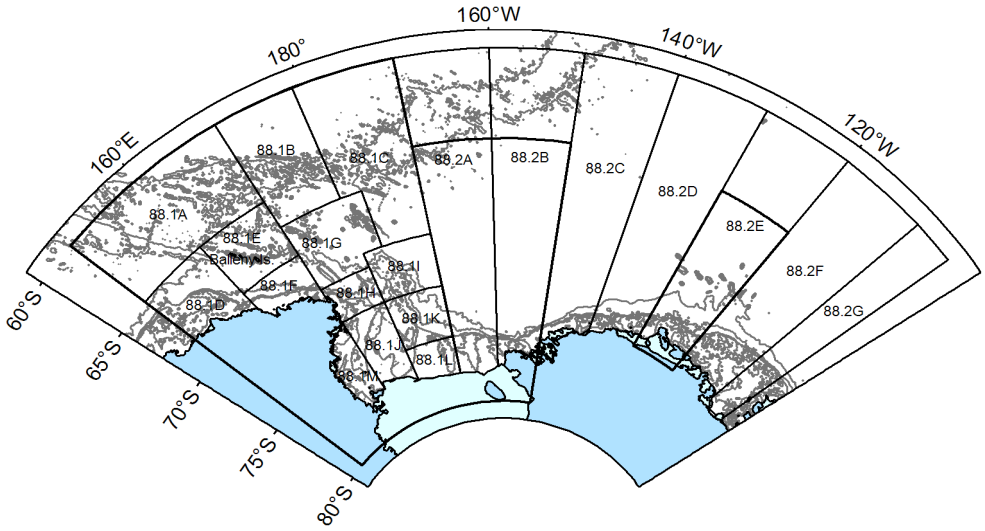

Figure 1: CCAMLR Subareas 88.1 and 88.2 and small scale statistical areas (SSRUs), showing the Ross Sea region and SSRU 882E (bounded regions). Depth contours plotted at 500, 1000, 2000, and 3000 m.

Dunn et al. (2004) introduced CASAL as a method for the assessment of Antarctic toothfish in the Ross Sea. In 2005, Dunn et al. (2005a) extended the model and also investigated an implementation of two and three area models, following the recommendations of SC-CAMLR-XXIII (2004). While Dunn et al. (2004) found that the single-area model of Antarctic toothfish fishery in the Ross Sea had some deficiencies in representing the observations, Dunn et al. (2005a) found that the data requirements of a multi-area model probably exceeded currently available information on movements and stock structure of Antarctic toothfish. However, they also found that, in a simulation experiment, a single-area model was likely to be conservative (i.e., estimates of current and equilibrium biomass were strongly biased low). Further, preliminary investigations of potential bias of tag based abundance estimators found, under simplistic assumptions of fish distribution, that the abundance estimates resulting from the current tagging program may have under-estimated the true abundance (Dunn et al. 2006). Initial investigation of the impact of the mixing assumption for tag data, using spatially explicit models, has begun using the Spatial

[1] Note that this report uses the CCAMLR split year that is defined from 1 December to 30 November. Hence, the term "year" refers to the fishing season in which most fishing occurs, e.g., the season from 1 December 1996 to 30 November 1997 is labelled as 1997.

Population Model (Dunn et al. 2009b). However analyses using that model have not yet been developed that would inform potential modifications to the Ross Sea assessment.

Here, we update the model of Dunn & Hanchet (2009b) by updating the catch for 2010 and 2011, catch-at-age frequencies for 2009 to 2010 (Stevenson et al. 2011), and the tag-release and recapture observations for 2010 and 2011 (Mormede et al. 2011a). We further update the model using tag data from the selected trips defined for the Ross Sea with the method outlined by Middleton (2009); and revised tag loss rates calculated by Dunn et al. (2011). In addition we present two sensitivities. In the first we explore the sensitivity of the model results to the inclusion of IUU catch and three levels of unaccounted mortality from Webber & Parker (2011). In the second we explore the sensitivity of the model results to the inclusion of the tag release and recapture data from all vessels.

2. METHODS

2.1 Population dynamics

In general, the Antarctic toothfish stock structure assumptions in this assessment were based on the 2009 base case presented by Dunn & Hanchet (2009b). The models were sex- and age-structured, with ages from 1–50, with the last age group a plus group (i.e., an aggregate of all fish aged 50 and older). The annual cycle was broken into three discrete time steps, nominally summer (November–April), winter (May–October), and end-winter (age-incrementation).

For each model run, the model structure and assumptions are described below. The CASAL input parameter files (`population.csl`, `estimation.csl`, and `output.csl`), selected output files (MPD estimates and MCMC estimates) for the model runs described below are available in the file (`Mormede_Ross_Sea_Assessment.zip`).

The models were run from 1995 to 2011, and were initialised assuming an equilibrium age structure at an unfished equilibrium biomass (i.e., a constant recruitment assumption) parameterised by the initial mid-season spawning stock biomass (SSB) and labelled B_0. Each model was implemented as a single-area, three-fishery model. Here, a single area was defined but the catch was removed using three concurrent fisheries (slope, shelf, and north, see Dunn et al. 2005b) with each fishery parameterised by a sex-based selectivity ogive, typically using double normal parameterisation (i.e., domed selectivity).

Recruitment was assumed to occur at the beginning of the first (summer) time step. Recruitment was assumed to be 50:50 male to female, and was parameterised as a year class strength multiplier (assumed to be equal to one for the years 1995–2011), multiplied by an average (unfished) recruitment (R_0) and a spawning stock-recruitment relationship (see later for the definition of the spawning stock biomass). The spawning stock-recruitment relationship was assumed to be a Beverton-Holt relationship with steepness of 0.75.

In all cases, selectivity coefficients for males at age were defined to have a range of 0–1, and female selectivity coefficients have range 0–a_{max} (where a_{max} was the value of the selectivity at the mode). Annual selectivity shifts for the slope and north fisheries were fitted that allowed the selectivity to 'shift' to the left or right with changes in the mean depth of the fishery for the slope and north fisheries. Annual selectivity shifts were not so constrained for the shelf, but were estimated as free parameters.

The double normal selectivity used to model the fishing selectivity for the reference model was parameterised using four estimable parameters a_1 (the mode), s_L (describes the shape of the left hand limb), s_R (describes the shape of the right hand limb) and a_{max} (value of the

selectivity at the mode). It had value equal to a_{max} at $x=a_1$, and $0.5a_{max}$ at $x=a_1-s_L$ or $x=a_1+s_R$, i.e., the value of the selectivity at age x was,

$$f(x) = a_{\max} \times 2^{-\left[(x-a_1)/s_L\right]^2}, \qquad (x \le a_1)$$
$$= a_{\max} \times 2^{-\left[(x-a_1)/s_R\right]^2}, \qquad (x > a_1)$$

To allow for differences in maximum selectivity by sex, the value of a_{max} was fixed at one for males, but allowed to be estimated for females. The selectivity shift was parameterised as $a_f\left(E_f - \overline{E}_f\right)$, where a_f was a shift factor and E_f was an exogenous variable (and was the catch-weighted mean depth fished of all sets with each year for the slope and north fisheries, expressed in units of years per 1000 m).

Natural mortality was assumed to be constant across age and sex classes, and the value of M assumed to be 0.13 y^{-1} (WG-FSA-SAM 2006).

Fishing mortality was applied only in the first (summer) time step from three concurrent fisheries. The process was to remove half of the natural mortality occurring in that time step, then apply the mortality from the fisheries instantaneously, then to remove the remaining half of the natural mortality. This differs from the more common Baranov catch equation, which implies that natural and fishing mortalities occur continuously and simultaneously. However, the difference in results from using either of these two catch equations was likely to be negligible. Hence, for each fishery f, an exploitation rate U_f was applied to the population, i.e.,

$$U_f = \frac{C_f}{\sum_{ij} \overline{w}_{ij} S_{ij} n_{ij} \exp\left(-0.5tM_{ij}\right)}$$

where C_f is the catch for fishery f, $\overline{w}_{ij}$ is the mean weight of fish of age i and sex j, S_{ij} is the selectivity at age i and sex j, n_{ij} is the number of fish, M_{ij} is the natural mortality, and t is the proportion of the year's natural mortality in the time step.

The maximum possible fishing pressure associated with f was defined as the maximum proportion of fish taken from any age/sex class in the area affected by fishery f (and constrained to be less than or equal to 0.999), i.e.,

$$\hat{U}_{\max}(f) = \max_{i,j}\left(S_{ij}U_f\right)$$

The population, n_{ij}, was then updated using

$$n'_{ij} = n_{ij} \exp\left(-tM_{ij}\right)\left(1 - S_{ij}U_f\right)$$

The models split the catch into three fisheries, defined as 'shelf', 'slope', and 'north'. The definitions of the areas that comprised the fisheries were based on stratifications derived from the tree based regression analysis of the catch-at-length data used to stratify the catch-at-age data by Hanchet et al. (2005) using the tree based regression method of Phillips et al. (2005). Shelf was defined as the SSRUs 88.1E–F, 88.1H–M, & 88.2A–B at a depth of less than 761 m; slope was defined as the SSRUs 88.1E–F, 88.1H–M, & 88.2A–B at a depth of greater than or equal to 761 m; and north was defined as SSRUs 88.1A–88.1C, and 88.1G. The suitability of these strata was confirmed using the catch-at-age data by Stevenson et al. (2011).

The annual reported catch for Antarctic toothfish in the Ross Sea, by area, for New Zealand vessels and for selected trips is given in Table 1. The total catch assumed for the north fishery of the Ross Sea in the 2011 season includes the 37 t reported by the *Insung No. 1* on the 5-day catch reports (see Stevenson et al. 2011 for details).

Estimated IUU catch for the Ross Sea is given in Table 2 (SC-CAMLR-XXIX 2011, Annex 4). Given the levels of historical IUU catch estimates for Subareas 88.1 and 88.2, the inclusion of IUU catch was unlikely to have any significant impact on the model estimates (see Dunn & Hanchet 2006, Dunn & Hanchet 2007), and we ignore it in the reference case model run. Possible unaccounted mortality from lost lines was estimated by Webber & Parker (2011), and is tabulated in Table 3. For years before 2007 where lost gear was not yet reported, an estimate of unaccounted mortality was made by back calculating using the mean annual unaccounted mortality rate during the four years for which the data were available. We ran sensitivity models assuming the catch included IUU catch, combined with the lower 10^{th} percentile, the mean, and the upper 90^{th} percentile estimates of unaccounted mortality.

Length-weight parameters are given in Table 4. The von Bertalanffy relationship was used to derive the mean length at age relationship (Table 4). Variability in the length at age relationship was parameterised by a normal distribution, with c.v. = 0.102 (Dunn et al. 2006).

We do not account for maturation in the sex-age structure of the population, but instead specify the time-invariant proportion of male and female fish at age that are mature. Hence, the mid-season spawning stock biomass (B) was determined as the biomass of the proportion of fish at age i and sex j considered mature, multiplied by the number of fish of age i and sex j after half of the natural mortality has been applied, evaluated in the second (winter) time step and summed over i and j, within a defined area.

Parker & Grimes (2009) determined that the mean age and length at 50% spawning for females on the Ross Sea slope region were 16.6 y or 133.2 cm and that the mean age and length at 50% spawning for males were 12.8 y or 120.4 cm. We use the spawning ogive of Parker & Grimes (2009) as the ogive for maturation in the assessment model (see Table 4), and hereafter use the term maturity ogive to describe this function.

In the age incrementation time step all fish age by 1 year, with the exception of fish in the 50 year plus group — these become the sum of all fish over 50 years and those aged 49.

The population model structure included tag-release and tag-recapture events. Here, the model replicated the basic age-sex structure described above for each tag-release event. The age and sex structure of the tag component was seeded by a tag release event. Tagging was applied to a 'cohort' of fish simultaneously (i.e., the 'cohort' of fish that were tagged in a given year and time step), and tagging from each year was applied as a single tagging event. The usual population processes (natural mortality, fishing mortality, etc.,) were then applied over the tagged and untagged components of the model simultaneously.

Table 1: Total reported Ross Sea Antarctic toothfish catch (t) for selected vessel trips and for all vessels, 1997–2011.

Year	Selected			All vessels			Total	Catch limit[1]
	Shelf	Slope	North	Shelf	Slope	North		
1997	0	0	0	0	0	0	0	1 980
1998	6	26	4	6	26	4	36	1 573
1999	0	0	0	14	282	0	296	2 281
2000	54	670	0	64	688	0	752	2 340
2001	113	347	132	113	347	132	592	2 314
2002	10	933	412	10	933	412	1 355	2 758
2003	2	608	996	2	609	1 158	1 769	4 135
2004	141	1 667	370	141	1 667	370	2 177	3 625
2005	230	1 839	513	397	2 262	550	3 210	3 625
2006	251	2 373	343	251	2 373	343	2 967	2 964
2007	28	1 886	572	68	2 438	573	3 079	3 072
2008	56	1 628	218	61	1 939	251	2 250	2 700
2009	62	1 185	276	135	1 904	393	2 432	2 700
2010	328	2 171	370	328	2171	370	2 868	2 850
2011	253	2 035	279	483	2052	347[2]	2 882	2 850
Total	1 533	17 366	4 486	2 072	19 690	4 904	26 666	

1. Catch limit for 88.1 and 88.2 *Dissostichus* spp. combined for the years 1997–2005, and for Subarea 88.1 and SSRUs 88.2A–B for 2006–2011.
2. In 2011, the *Insung No. 1* did not report any catch on the C2 forms. We supplemented the C2 reported catch totals with the 37 tonnes reported by the *Insung No. 1* using 5-day catch reports. As the catch from the *Insung No. 1* was taken from the northern SSRUs, we allocated its catch to the North region.

Table 2: Total IUU catch of Dissostichus spp. for Subareas 88.1 & 88.2, for the years 1997–2011 (source: SC-CAMLR-XXIX 2011, Annex 4 for 1997–2010; D. Ramm, CCAMLR Secretariat, pers. comm. for 2011).

Year	Subarea 88.1	Subarea 88.2	Total
1997	0	0	0
1998	0	0	0
1999	0	0	0
2000	0	0	0
2001	0	0	0
2002	92	0	92
2003	0	0	0
2004	240	0	240
2005	23	0	23
2006	0	15[1]	15
2007	0	0	0
2008	186	0	186
2009	0	0	0
2010	0	0	0
2011	0	0	0
Total	360	15	375

1. Associated with SSRU 88.2A, and hence assumed to be a catch in the Ross Sea region.

Table 3: Estimated unaccounted mortality for *Dissostichus mawsoni* in the Ross Sea arising from lost lines, 1998–2011.

Year	Catch	Unaccounted mortality								
		10th percentile			Mean			90th percentile		
		Catch	%	Total	Catch	%	Total	Catch	%	Total
Shelf										
1998	6	0.1	1.5	6	0.2	3.4	6	0.3	5.6	6
1999	14	0.2	1.5	15	0.5	3.4	15	0.8	5.6	15
2000	64	1.0	1.5	65	2.2	3.4	67	3.6	5.6	68
2001	113	1.7	1.5	114	3.9	3.4	116	6.3	5.6	119
2002	10	0.2	1.5	10	0.3	3.4	10	0.6	5.6	11
2003	2	0.0	1.5	2	0.1	3.4	2	0.1	5.6	2
2004	141	2.2	1.5	143	4.8	3.4	145	7.9	5.6	148
2005	397	6.1	1.5	403	13.7	3.4	411	22.3	5.6	420
2006	251	3.9	1.5	255	8.7	3.4	259	14.1	5.6	265
2007	68	1.0	1.5	69	2.3	3.4	70	3.8	5.6	71
2008	61	0.0	0.0	61	0.0	0.0	61	0.0	0.0	61
2009	135	0.1	0.1	135	0.1	0.1	135	0.2	0.1	135
2010	328	20.0	6.1	348	45.0	13.7	373	73.0	22.3	401
2011	483	0.0	0.0	483	0.0	0.0	483	0.0	0.0	483
Slope										
1998	26	0.8	3.1	27	1.1	4.2	27	1.4	5.3	27
1999	282	8.9	3.1	291	11.8	4.2	294	14.9	5.3	297
2000	688	21.6	3.1	710	28.8	4.2	717	36.3	5.3	724
2001	347	10.9	3.1	358	14.6	4.2	362	18.3	5.3	365
2002	933	29.3	3.1	962	39.1	4.2	972	49.3	5.3	982
2003	609	19.1	3.1	628	25.5	4.2	635	32.2	5.3	641
2004	1 667	52.3	3.1	1 719	69.9	4.2	1 737	88.0	5.3	1 755
2005	2 262	71.0	3.1	2 333	94.9	4.2	2 357	119.5	5.3	2 381
2006	2 373	74.5	3.1	2 448	99.5	4.2	2 473	125.3	5.3	2 498
2007	2 438	76.6	3.1	2 515	102.2	4.2	2 540	128.8	5.3	2 567
2008	1 939	56.0	2.9	1 995	78.0	4.0	2 017	100.0	5.2	2 039
2009	1 904	46.0	2.4	1 950	57.0	3.0	1 961	68.0	3.6	1 972
2010	2 171	148.0	6.8	2 319	197.0	9.1	2 368	249.0	11.5	2 420
2011	2 052	9.0	0.4	2 061	14.0	0.7	2 066	19.0	0.9	2 071
North										
1998	4	0.7	18.1	5	1.0	26.2	5	1.4	34.5	5
1999	0	0.1	18.1	1	0.1	26.2	1	0.1	34.5	1
2000	0	0.0	18.1	0	0.0	26.2	0	0.0	34.5	0
2001	133	24.0	18.1	157	34.7	26.2	167	45.8	34.5	178
2002	412	74.7	18.1	487	108.0	26.2	520	142.3	34.5	554
2003	1 158	210.1	18.1	1 368	303.7	26.2	1 462	400.0	34.5	1 558
2004	370	67.1	18.1	437	97.0	26.2	467	127.7	34.5	498
2005	550	99.8	18.1	650	144.3	26.2	694	190.0	34.5	740
2006	343	62.3	18.1	406	90.0	26.2	433	118.6	34.5	462
2007	573	104.0	18.1	677	150.3	26.2	723	198.0	34.5	771
2008	251	91.0	36.3	342	117.0	46.6	368	142.0	56.6	393
2009	393	52.0	13.2	445	74.0	18.8	467	97.0	24.7	490
2010	370	31.0	8.4	401	66.0	17.8	436	104.0	28.1	474
2011	347	51.0	14.7	398	75.0	21.6	422	100.0	28.8	447

Table 4: The 2011 reference model biological parameters (natural mortality, growth, length-weight relationship, and length or age at maturity).

Relationship	Parameter	Value	
		Male	Female
Natural mortality	M (y^{-1})	0.13	0.13
Von Bertalanffy	t_0 (y)	-0.256	0.021
	k (y^{-1})	0.093	0.090
	L_∞ (cm)	169.07	180.20
	c.v.	0.102	0.102
Length-weight	a ($t.cm^{-1}$)	1.387e-008	7.154e-009
	b	2.965	3.108
Age at maturity (y)	A_{50} ($\pm A_{to95}$)	12.79 (±3.51)	16.58 (± 7.32)

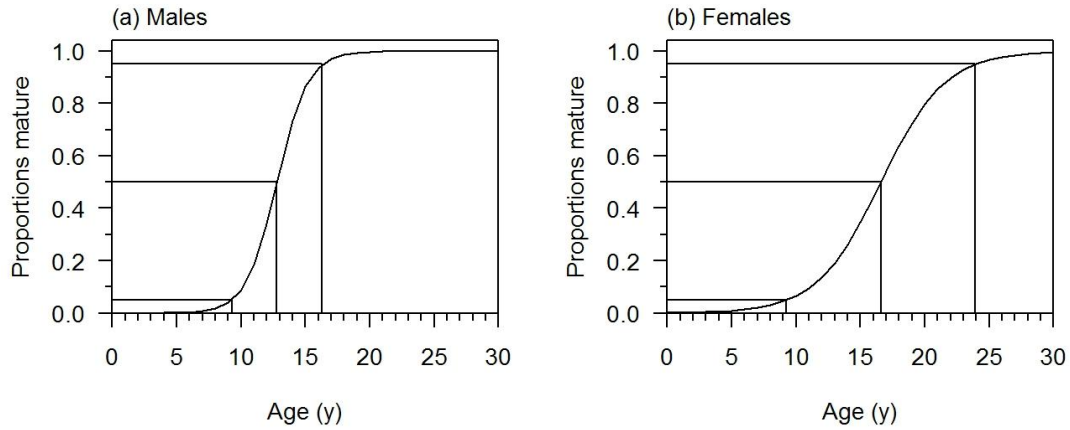

Figure 2: The assumed maturity ogive (Parker & Grimes 2009) by age for (a) males, and (b) females.

2.2 Model estimation

The model parameters were estimated by minimising an objective function, which is the sum of the negative log-likelihoods from the data, negative-log priors (in a Bayesian analysis), and penalties that constrain the parameterisations, i.e., the objective function in a Bayesian analysis for **p**, the vector of the free parameters, L the likelihood function, and O_i the ith observation was

$$\text{Objective } (\mathbf{p}) = -\sum_i \log\left[L(\mathbf{p} \mid O_i)\right] - \log\left[\theta(\mathbf{p})\right]$$

Where θ is the joint prior (and penalty) density of the parameters **p**. The observations, likelihoods, penalties, and priors are described below.

Initial model fits were evaluated at the maximum of the posterior density (MPD), MPD profile distributions (i.e., by evaluating the minimum objective function while fixing one parameter and allowing all other parameters to vary), and model fits and residuals. At the MPD, the approximate covariance matrix of the free parameters was calculated as the inverse of the approximation to the Hessian, and the corresponding correlation matrix also calculated.

To estimate the joint posterior distribution of the parameters in a Bayesian analysis, CASAL uses a straightforward implementation of the Metropolis algorithm (Gelman et al. 1995, Gilks

et al. 1998) to execute the Monte Carlo Markov Chain (MCMC). The Metropolis algorithm attempts to draw a sample from a Bayesian posterior distribution, and calculates the posterior density π, scaled by an unknown constant. The algorithm generates a 'chain' or sequence of values. Typically the beginning of the chain is discarded and every nth element of the remainder is taken as the posterior sample. The chain is produced by taking an initial point x_0 and repeatedly applying the following rule, where x_i is the current point; (i) draw a candidate step s from a proposal distribution J, which should be symmetric i.e., $J(-s)=J(s)$, (ii) calculate $r=\min(\pi(x_i + s) / \pi(x_i),1)$, and (iii) let $x_{i+1}=x_i + s$ with probability r, or x_i with probability $1-r$.

A point estimate (i.e., the MPD) was produced, along with the approximate covariance matrix of the parameters (as the inverse Hessian) (see Bull et al. 2008, for more detail), and used as the starting point for the chain.

MCMCs were estimated using a burn-in length of $5\text{x}10^5$ iterations, with every 1000^{th} sample taken from the next $1\text{x}10^6$ iterations (i.e., a systematic sample of length 1000 was taken from the Bayesian posterior). Chain diagnostic plots, autocorrelation estimates, and single chain convergence tests of Geweke (1992) and Heidelberger & Welch (1983) stationarity and half-width were used to determine evidence of non-convergence. The tests used a significance level of 0.05 and the diagnostics were calculated using the Bayesian Output Analysis software (Smith 2003).

2.3 Observations

2.3.1 Proportions-at-age in the catch

The catch proportions-at-age data were fitted to the modelled proportions-at-age composition using a multinomial likelihood, i.e.

$$-\log(L) = -\log(N!) + \sum_i \left[\log\left((NO_i)!\right) - NO_i \log(E_i) \right]$$

where N is the effective sample size, O_i are the observed proportions-at-age i, and E_i are the model expected proportions-at-age i. Proportions-at-age data were derived from the aged otoliths collected by observers and the length frequency of the catch. Stevenson et al. (2011) described the catch-at-age data available for the assessment models, with data available for the years 1998–2010. Otolith data for the 2011 season were unavailable at the time of this report, and hence age data for 2011 are not included within the assessment models. The effective sample sizes assumed for the proportions-at-age data are described below.

Annual selectivity shifts were estimated in the models. For the slope and north fisheries the annual selectivity was based on a multiplier of the mean depth fished (weighted by the catch) from all sets within each fishery in each year (Table 5). For the shelf fishery, independent annual selectivity shifts were estimated for the shelf fishery selectivities.

Ageing error was accounted for by modifying the likelihoods for the proportions-at-age data such that E_i was replaced by E'_i, where E'_i were the expected proportions-at-age multiplied by a ageing error misclassification matrix A. The error misclassification matrix was derived from a normal distribution with constant c.v. = 0.1 (P. Horn, NIWA, pers. comm.).

Table 5: Weighted mean depth (m), and the average depth fished by fishery (shelf, slope, and north), for the years 1998–2011.

Year	Shelf	Slope	North	All fisheries
1998	702	982	775	912
1999	671	916	571	904
2000	717	974	–	952
2001	654	1 243	1 184	1 118
2002	738	1 118	1 403	1 202
2003	691	1 372	1 477	1 440
2004	662	1 231	1 353	1 215
2005	638	1 199	1 463	1 174
2006	654	1 208	1 379	1 181
2007	658	1 190	1 483	1 233
2008	716	1 206	1 528	1 229
2009	721	1 163	1 617	1 212
2010	699	1 164	1 456	1 149
2011	715	1 102	1 661	1 097
Mean	682	1 175	1 469	1 209

2.3.2 Tag-release data

Tag-release data are not technically observations within the models, but rather non-estimable parameters. Numbers of available individual fish tagged and released for New Zealand vessels were initially described by Dunn et al.(2005c), and updated for 2007 by Dunn et al. (2007), for 2009 by Dunn et al. (2009a), and in 2011 by Mormede et al. (2011a). Tag-release events were defined for 2001–2010 and within-season recaptures were ignored (Table 6), with the number released assumed to be the number of fish tagged less the number recaptured within-season for each year. Tag release events were assumed to have occurred at the end of the first (summer) time step, following the (summer) natural and fishing mortality.

Each season's tag-release data was included as a separate member of the model structure, i.e., the model kept account of the numbers of fish tagged in each year separately. Initial tag mortality was assumed to be 10% (Agnew et al. 2005) plus initial tag loss, effectively reducing the number of tagged fish in the population at the time they were tagged.

Instantaneous tag-loss was assumed to occur in equal proportions in the first two time steps, but not in the third. Here, the number of fish in each tagged cohort at time j (i.e., the number n_{ij} in any age/sex element i of the population at time step j) was determined by applying the tag loss rate for that cohort, l_i, by the proportion of tag loss to apply in that time step t_j, i.e.

$$n'_{ij} = n_{ij} \exp\left(-t_j l_i\right)$$

Dunn et al. (2011) showed that the loss rate for double tags in the assessment models of Dunn & Hanchet (2009a, 2009b) had been incorrectly derived and applied, with the effect that loss rates were slightly over-estimated for double tagged fish in the first four years and under-estimated after that. Tag loss rate and the double tag approximation rates were re-estimated by Dunn et al. (2011) using a much larger data set. They estimated the loss rate as $\lambda = 0.0084\ y^{-1}$ when excluding recapture events that occurred after six years at liberty. Dunn et al. (2011) showed that the impact on the assessment of ignoring tag recapture data after a six year period removed a small positive bias at the expense of increasing variance by a small amount (<1% change in the overall mean squared error). Hence, we assume a tag loss rate of $\lambda = 0.0084\ y^{-1}$

for double tagged fish and ignore recaptures that occurred after six years at liberty in the base case model.

Dunn et al. (2005c) showed that tagging appears to result in a check on growth of individual fish. We assume that the effect of tagging on growth is equivalent to a short period of 'no growth' when fish are tagged by adjusting the t_0 von Bertalanffy growth parameter by -0.5 years (Dunn & Hanchet 2007). Here, the effective size at age for a tagged fish is the same as the size at age for an untagged fish at that age less 0.5 years, i.e., the mean size at age for a tagged fish was modelled as,

$$\bar{s}\left(age\right) = L_{\inf}\left(1-\exp\left(-k\left(age-t_0-g_i\right)\right)\right),$$

where g_i=0.5.

In all cases, the numbers of tagged fish at age were calculated deterministically from the observations of numbers of fish at length. A selectivity was applied to the conversion of fish-at-length to fish-at-age within each fishery, i.e., for each of the shelf, slope, and north fisheries separate tag release events were specified for each year along with the appropriate fishing selectivity. Hence, the numbers of fish tagged at age were determined from the selected length frequency of the untagged fish, the length frequency of tagged fish, and the population state and parameters in the given year and time step of the release event.

2.3.3 Tag-recapture observations

Numbers of tagged fish recaptured are given by Mormede et al. (2011a), and summarised in Table 6. Following Dunn et al. (2005b), we ignored within-season recoveries, and only used data from the between-season recaptures. The estimated number of scanned fish (i.e., those fish that were caught and inspected for a possible tag) was derived from the sum of the scaled length frequencies from the vessel observer records plus the numbers of fish tagged and released less those tags recaptured within-season. Tag recapture events were assumed to occur at the end of the first (summer) time step. Detection probabilities for Antarctic toothfish in the Ross Sea are thought to be 100% (Dunn & Hanchet 2007). However, a small number of unlinked tags were found in the tag recapture data (Mormede et al. 2011b). For Antarctic toothfish in the Ross Sea, a total of 18 of the 1487 tags were unlinked, i.e., 1.2% of recaptures. Hence to account potential tags that are unlinked, we assume a tag detection rate of 98.8%.

For each year, the recovered tags at length for each release event t were fitted, in 10 cm length classes (range 40–230 cm), using a binomial likelihood, i.e.,

$$-\log\left(L\right) = \sum_i \left[\log\left(n_i!\right) - \log\left(\left(n_i-m_i\right)!\right) - \log\left(m_i!\right) + m_i \log\left(\frac{M_i}{N_i}\right) + \left(n_i-m_i\right)\log\left(1-\frac{M_i}{N_i}\right)\right]$$

where n_i=number of fish in length class i that were scanned, m_i=number of tagged fish in length class i that were recaptured from the release event t, N_i=expected number of fish in length class i in the population, and M_i=expected number of fish in length class i in the tagged population from t.

Table 6: Numbers of Antarctic toothfish with tags released for the years 2001–2011 for (a) selected trips, (b) all trips, and the number recaptured in 2002–2011. Numbers in italics correspond to fish which have been at liberty for over six years.

Data		Released fish	Recaptures										
	Year	Number	2002	2003	2004	2005	2006	2007	2008	2009	2010	2011	Total
Selected trips	2001	259	1	1	0	0	0	1	*1*	*1*	*0*	*0*	5
	2002	684	2	5	4	9	8	13	6	*4*	*2*	*5*	58
	2003	844	–	7	10	8	2	9	2	2	*2*	*2*	44
	2004	2 030	–	–	7	21	19	32	23	8	14	*10*	134
	2005	2 914	–	–	–	8	26	26	28	5	47	13	153
	2006	3 023	–	–	–	–	11	86	47	12	28	19	203
	2007	2 780	–	–	–	–	–	14	52	17	49	21	153
	2008	2 125	–	–	–	–	–	–	12	10	35	18	75
	2009	1 791	–	–	–	–	–	–	–	1	38	27	66
	2010	3 064	–	–	–	–	–	–	–	–	27	57	84
	2011	2 766	–	–	–	–	–	–	–	–	–	12	12
	Total	22 280	3	13	23	47	68	181	172	60	143	184	994
All trips	2001	259	1	1	0	0	0	1	*1*	*1*	*0*	*0*	5
	2002	684	2	5	4	9	8	13	6	*5*	*2*	*5*	59
	2003	846	–	7	10	8	2	9	2	2	*2*	*2*	44
	2004	2 030	–	–	7	21	19	32	26	12	14	*10*	141
	2005	3 271	–	–	–	8	26	29	30	11	47	14	165
	2006	3 023	–	–	–	–	11	89	68	15	28	20	231
	2007	3 524	–	–	–	–	–	18	62	22	50	25	177
	2008	2 495	–	–	–	–	–	–	14	19	36	18	87
	2009	2 828	–	–	–	–	–	–	–	9	41	36	86
	2010	3 064	–	–	–	–		–	–	–	27	58	85
	2011	3 034	–	–	–	–		–	–	–	–	12	12
	Total	25 058	3	13	21	46	66	191	209	96	247	200	1 092

2.3.4 Process error and data weighting

Additional variance, assumed to arise from differences between model simplifications and real world variation, was added to the sampling variance for all observations. Adding such additional errors to each observation type has two main effects, (i) it alters the relative weighting of each of the data sets (observations) used in the model, and (ii) it typically increases the overall uncertainty of the model, leading to wider credible bounds on the estimated and derived parameters.

The additional variance, termed process error, was estimated for each model MPD run, and for each model, the total error assumed for each observation was calculated by adding process error and observation error. A single process error was estimated for each of the observation types (i.e., one for the age data and one for the tag data), with the procedure for calculating the additional process error as described below.

Estimates of the sample size for the proportions-at-age observations were made via a two-step process. First, the sample sizes were derived by assuming the relationship between the observed proportions, E_i, and estimated c.v.s, c_i, followed that for a multinomial distribution with unknown sample size N_j. The estimated sample size was then derived using a robust non-linear least squares fit of $\log(c_i) \sim \log(P_i)$. Second, estimates of the effective sample size, N_j', by adding additional process error, N_{PE}, to the sample size calculated above, where,

$$N'_j = 1 \Big/ \left(1/N_j + 1/N_{PE} \right)$$

i.e., from an initial MPD model fit, an estimate of the additional process error was made by solving the following equation for N_{PE},

$$n = \sum_{ij} \frac{\left(O_{ij} - E_{ij}\right)^2}{E_{ij}\left(1/N_j + 1/N_{PE}\right)}$$

where n was the number of multinomial cells, O_{ij} was the observed proportions for age class i in year j, E_{ij} was the expected proportions, N_j was the effective sample size estimated above, and N_{PE} was the associated process error for that class of observations.

Estimates of the over-dispersion for the tag-recapture likelihoods were made using a similar method to that for the proportions-at-age data. First, initial sample sizes for the numbers recaptured and the numbers scanned were assumed from the actual numbers recaptured and numbers scanned. Second, the over-dispersion ϕ_j for each tagging event was calculated from its i recapture events, from an initial MPD run, where,

$$\phi_j = \mathrm{var}\left(\frac{O_{ij} - E_{ij}}{\sqrt{E_{ij}(1 - p_{ij})}}\right)$$

where O_{ij} was the observed number of recaptures, E_{ij} the expected number of recaptures, and p_{ij} the expected probability of recapture. Over-dispersion terms for each of the recapture events were then combined (i.e., by taking the geometric mean), and the log-likelihood was then modified by multiplying by $1/\phi$.

The process error was estimated to $N_{PE} = 171$ and $\phi = 1.213$ for the base case model. Process error estimates for the sensitivity models had very similar values. Process error estimates for the sensitivity models are given in Section 2.7.

2.4 Penalties

Two types of penalties were included within the model. First, the penalty on the catch constrained the model from returning parameter estimates where the population biomass was such that the catch from an individual year would exceed the maximum exploitation rate (see earlier). Second, a tagging penalty discouraged population estimates that were too low to allow the correct number of fish to be tagged. However, in the model runs presented here, these penalties had no significant contribution to the total likelihood.

2.5 Priors

Priors were defined for all free parameters in the models. The free parameters, starting values for the minimisation, and bounds are given below in Table 7. In models presented here, priors were chosen so that they were relatively non-informative but also encouraged lower estimates of B_0. Note that the priors for the parameters were, in general, set to be the same as for the 2009 models (Table 7).

Table 7: Number (*N*), start values, priors, and bounds for the free parameters (when estimated) for the model runs.

Parameter		*N*	Start value	Prior	Bounds	
					Lower	Upper
B_0		1	80 000	Uniform-log	$1x10^4$	$1x10^6$
Male fishing selectivities	a_1		8.0	Uniform	1.0	50.0
	s_L		4.0	Uniform	1.0	50.0
	s_R	9	10.0	Uniform	1.0	500.0
Female fishing	a_{max}		1.0	Uniform	0.01	10.0
selectivities	a_1		8.0	Uniform	1.0	50.0
	s_L		4.0	Uniform	1.0	50.0
	s_R	12	10.0	Uniform	1.0	500.0
Selectivity shift (ykm^{-1})	a_f	2	1.0	Uniform	0.0	20.0
Annual selectivity shift[1]	E_f	14	Mean depth	Uniform	-10.0	10.0

2.6 Yield calculations

Yield estimates were calculated by projecting the estimated current status for each model under a constant catch assumption using the rules,

- $Rule_1$: Choose a yield γ_1 so that the probability of the spawning biomass dropping below 20% of its median pre-exploitation level over a 35-year harvesting period is 10% (depletion probability).
- $Rule_2$: Choose a yield γ_2 so that the median escapement at the end of a 35-year period is 50% of the median pre-exploitation level.
- $Rule_3$: Select the lower of γ_1 and γ_2 as the yield.

The probability of depletion and the level of escapement were calculated by projecting forward for a period of 35 years under a scenario of a constant annual catch (i.e., for the period 2012–2047), for each sample from the posterior distribution. The depletion probability was calculated as the proportion of samples from the Bayesian posterior where the predicted future SSB was below 20% of B_0 in that respective sample in at least one year for each year over a 35-year projected period. The level of escapement was calculated as the proportion of samples from the Bayesian posterior where the predicted future SSB was below 50% of B_0 in that respective sample at the end of a 35-year projected period. The posterior sample estimates of B_0 were used as a proxy for the pre-exploitation median SSB in each sample. Note that the use of the B_0 proxy will result in a small downward bias of the stock status in each trial and hence a small downward bias in the estimate of yield.

For the yield calculations, recruitment for the years 2003–2046 was assumed to be lognormally distributed with a standard deviation of 0.6 (Dunn & Hanchet 2006); future catch was assumed to follow the same split between fisheries as that in the four most recent seasons (i.e., based on the distribution of the 2009–2011 catch, 11.3%, 75.4%, and 13.3% of the total future catch was allocated to the shelf, slope, and north fisheries respectively); and that the selectivity shifts were assumed to be the mean of those estimated for the years 1998–2011. Note that since 2009, a higher proportion of the total catch has been taken from the shelf than in the years immediately before (i.e., the future allocation was previously assumed to be 3.5%, 81.2%, and 15.3% for the shelf, slope, and north fisheries respectively).

The decision rules were evaluated under two scenarios, (i) assuming that the future constant catch was equal to the 2010 and 2011 catch limits (CM41-09, SC-CAMLR-XXVIII 2009), and (ii) the maximum future constant catch that met the decision rule criteria. Note that, in previous years in the Ross Sea fishery, the total catch limit has not always been taken. Ice cover over fishable depths in the southern SSRUs has meant that fishing vessels were unable

to access some of the available catch. We ignore possible ice cover restrictions on future catch, and assume that for each future season, the available catch would be taken, subject to the maximum exploitation rate rule (U_{max}=0.999).

2.7 Model runs

The 2011 reference case model was essentially an update of the 2009 base case. It used the tag data from selected vessels only, based on the selection method of Middleton (2009). The data set selection first defined an informative data set based on trips that were both (i) vessel trips in a single year whose tags were subsequently recovered at a rate above the median rate for all trips undertaken in that year, and (ii) vessel trips in a single year which recovered tags at a rate above the median rate for all trips undertaken in that year. A selected data set was then defined as all trips that had data quality metrics that were within the established bounds for the data-quality metrics for the trips that met criteria (i) and (ii) above.

In addition to the 2011 reference case (R1), we investigate the following sensitivity analyses: (i) the same as the 2011 reference case but with the inclusion of IUU catch and then three alternative assumptions of the level of unaccounted mortality based on the estimates of Webber & Parker (2011) (R2.1, R2.2, and R2.3); and (ii) the same as the 2011 reference case but using the tag release and recapture data from all vessel trips (R3). The reference case and the sensitivity model runs are summarised in Table 8. We present the MCMC estimates for only one of the sensitivity models with unaccounted mortality, where we assume the 90th percentile estimate. This choice was because this represents the 'worst' case scenario. The other two models (10th percentile and the mean) will give estimates on initial biomass, current biomass, and yield that lie between the 90th percentile unaccounted mortality case and the 2011 reference case.

Table 8: Labels and description of the model runs.

Model	Description
	The 2009 base case (Dunn & Hanchet 2009b)
R1	2011 reference case (the 2011 implementation of the 2009 base case)
R2.1	Model R1, but including IUU and the 10th percentile estimate of unaccounted mortality
R2.2	Model R1, but including IUU and the mean estimate of unaccounted mortality
R2.3	Model R1, but including IUU and the 90th percentile estimate of unaccounted mortality
R3	Model R1, but using the tag release and recapture data from all vessel trips

Table 9: Process error estimates for catch-at-age (N_{PE}) and tag-recapture ($\varnothing$) observations for the 2011 reference model and the sensitivity models (models R1–R3).

Model		N_{PE}	$\varnothing$
R1	2011 reference case	171	1.213
R2.1	10th percentile unaccounted mortality	175	1.204
R2.2	Mean unaccounted mortality	175	1.204
R2.3	90th percentile unaccounted mortality	175	1.204
R3	All vessel trips	171	1.286

3. RESULTS

3.1 MPD results

Objective function values for the MPD estimates for the model runs are given in Table 10 and estimates of initial (B_0) and current biomass given in Table 11. Comparison of the objective function values suggested that there were only minor differences in fit between each of the data sets in each of the model runs. Likelihood values were similar across all of the models

The estimated value of the initial biomass for model R1 (the reference case) gave an estimate of the initial biomass of 73 810 t. Model diagnostics did not suggest any evidence of poor fit to the observations (Table 10). Models R2.1, R2.2, and R2.3 that assumed some unaccounted mortality suggested a similar initial biomass but a slightly faster decline, where assumptions of an increased uncounted mortality led to slightly faster declines. The largest difference was for model R2.3, for which B_{2011} was estimated to be 77.6% of B_0. Model R3 suggested a higher initial biomass (85 710 t) than the other models.

Table 10: MPD objective function values and number of estimated parameters for all model runs.

Objective function	Model run				
Component	R1	R2.1	R2.2	R2.3	R3
2001 tags recaptured	10.9	10.9	10.9	10.9	10.3
2002 tags recaptured	61.4	61.9	62.0	62.0	56.6
2003 tags recaptured	67.7	68.2	68.1	68.2	63.3
2004 tags recaptured	100.7	101.7	101.8	101.8	94.0
2005 tags recaptured	106.3	107.2	107.3	107.3	102.3
2006 tags recaptured	113.3	114.3	114.3	114.3	122.6
2007 tags recaptured	92.6	93.5	93.7	93.7	87.2
2008 tags recaptured	44.1	44.6	44.6	44.6	44.0
2009 tags recaptured	30.5	30.8	30.8	30.8	28.8
2010 tags recaptured	18.6	18.7	18.7	18.7	18.9
Catch-at-age (North)	698.1	702.2	701.9	702.0	698.0
Catch-at-age (Shelf)	792.5	799.6	799.9	799.9	791.5
Catch-at-age (Slope)	951.9	960.2	960.1	960.1	951.9
Sub-total (observations)	3088.6	3113.4	3114.0	3114.2	3069.5
Penalties	0.0	0.0	0.0	0.0	0.0
B_0 prior	11.2	11.2	11.2	11.2	11.4
All other priors	0.0	0.0	0.0	0.0	0.0
Total objective function	3099.8	3124.6	3125.2	3125.4	3080.8
No. of free parameters	36	36	36	36	36

Table 11: Selected MPD parameter values for the 2009 base case (Dunn & Hanchet 2009b) and 2011 model runs R1–R3.

Model		B_0	B_{2009}	B_{2009} (%B_0)	B_{2011}	B_{2011} (%B_0)
	2009 base case	62 340	52 160	83.7	–	–
R1	2011 reference case	73 810	61 510	83.3	59 030	80.0
R2.1	10^{th} percentile unaccounted mortality	74 230	60 840	82.0	58 310	78.6
R2.2	Mean unaccounted mortality	74 430	60 419	81.2	57 799	77.7
R2.3	90^{th} percentile unaccounted mortality	74 440	60 420	81.2	57 780	77.6
R3	All vessel trips	85 710	73 390	85.6	70 910	82.7

3.2 Retrospective model runs excluding 2010 and 2011 tag recapture data

A retrospective analysis was run on the 2011 reference case to investigate reasons for difference in the estimates of initial biomass between the 2009 base case and the 2011 reference case. First, we excluded the 2011 observations from model R1 (labelled model R1.1), and then excluded the 2010 and 2011 observations (labelled model R1.2). Estimates of initial and current biomass are given in Table 12. The retrospective models suggested that about 45% of the increase in the estimated initial biomass between the 2009 base case and the 2011 reference case was due to the change in tag recapture data associated with the changed selection of vessel trips; 35% was due to the influence of the 2011 tag recapture observations, and the remaining 20% to the influence of the 2010 tag recapture observations. With more years of data available, the trip selection method included a larger proportion of all vessel trips — up from 65% of all vessel trips selected in 2009 to 85% of vessel trips in 2011.

In order to investigate the effects of different vessel trip selection algorithms, we considered the case where we ignore the first year's data from every vessel when deriving the selected vessel trips. For example, in 2011, five vessels fished that had no previous history in the Ross Sea fishery; and of these, three were included by the select algorithm. We developed a modification to the select method where vessels were excluded in their first fishing season (labelled model R1.3). While this reduced the size of the select vessel trips to about 59% of all trips, estimates of initial biomass (71 250 t) were similar to the 2011 reference case (73 810 t). Model R1.3 also appeared more consistent in the retrospective analysis, with model runs excluding either the 2011 (R1.31) or the 2010/2011 (R1.32) observations alone returning very similar estimates of initial biomass. This would suggest that the change between the 2009 and 2011 models is likely to be due to the selected vessel trips that were included by the algorithm, interacting with the additional tag-recapture and release observations for 2010 and 2011.

Table 12: Selected MPD parameter values for the reference case (R1) and the retrospective analyses.

Model		B_0	B_{2009}	B_{2010}	B_{2011}
R1	2011 reference case	73 810	61 510	60 200	59 030
R1.1	Excluding 2011 observations	69 550	57 240	55 930	54 770
R1.2	Excluding 2010 and 2011 observations	67 160	54 850	53 550	52 380
R1.3	Excluding first occurrence of vessels	71 250	58 920	57 620	56 480
R1.31	R1.3 excluding 2011 observations	70 190	57 860	56 560	55 400
R1.32	R1.3 excluding 2010 and 2011 observations	70 170	57 830	56 530	55 370

3.3 Likelihood profiles

Likelihood profiles for models R1, R2.3, and R3 (2011 reference case, IUU and 90th percentile unaccounted mortality, and all vessel trips) are given below (Figures 3–5). For all models, likelihood profiles were carried out by fixing B_0 at values across a range of values (i.e., 40 000–120 000 t in the examples below), with the remaining parameters estimated.

The likelihood profiles for all three models showed similar trends. The catch-at-age data and tag recaptures from 2003, 2005, and 2008 suggested that very low biomass levels were less likely, whilst tag recaptures from 2002, 2006, and 2007 suggested that very high biomass estimates were less likely, as with the 2009 base case model. The tag recaptures from 2009 and 2010 provided little additional information on the initial biomass. As in previous assessments, the profiles were influenced by the shelf catch-at-age proportions, suggesting that very low estimates of initial biomass were less likely. However, unlike in 2009, the tag recapture observations dominated the likelihoods at the lower end.

The likelihood profiles for models R3 (all vessels, Figure 5)showed that the influence of the tag recapture data for 2002 and 2007 was much weaker, leading to higher estimate of initial biomasses — a consequence of the larger number of samples of tag data in these models.

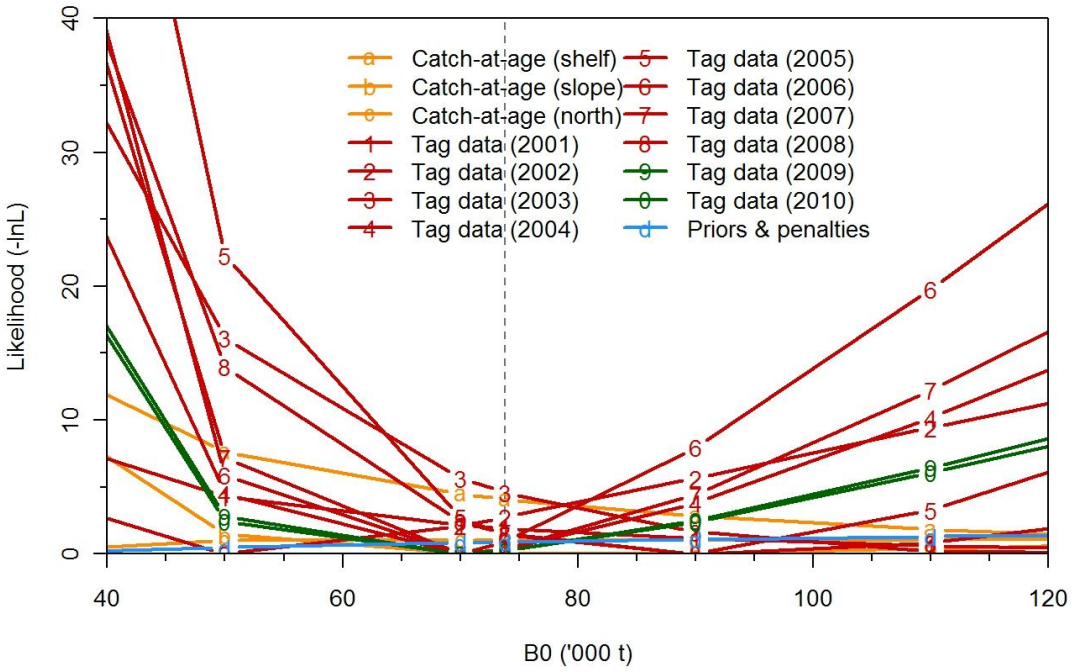

Figure 3: Likelihood profiles for model R1 (2011 reference case) of B_0. Negative log likelihood values rescaled to have minimum 0 for each data set. The dashed vertical line indicates the MPD.

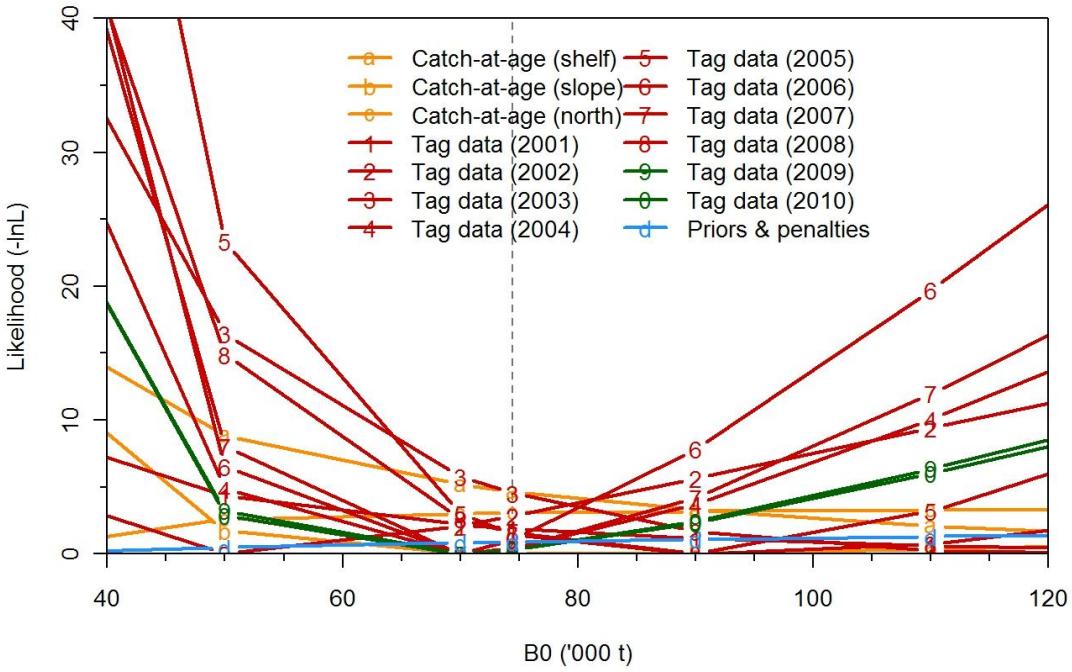

Figure 4: Likelihood profiles for model R2.3 (selected trips tag data and IUU and 90th percentile unaccounted mortality) of B_0. Negative log likelihood values rescaled to have minimum 0 for each data set. The dashed vertical line indicates the MPD.

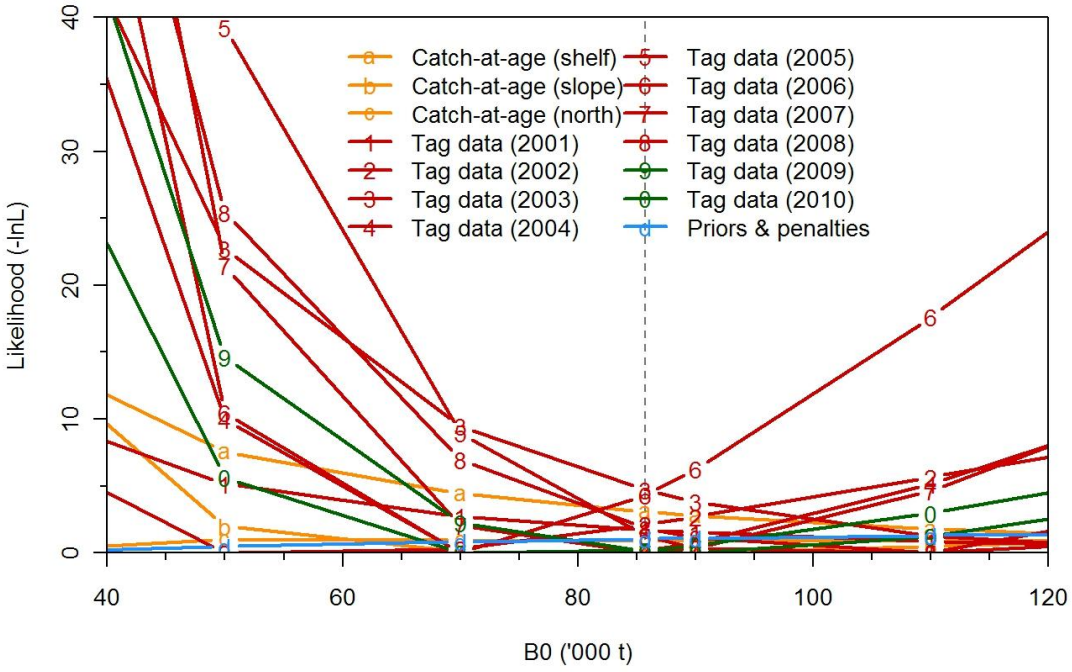

Figure 5: Likelihood profiles for model R3 (all vessels tag data) of B_0. Negative log likelihood values rescaled to have minimum 0 for each data set. The dashed vertical line indicates the MPD.

3.4 MCMC results

3.4.1 MCMC diagnostics

Trace plot diagnostics of key parameters (B_0 and B_{2011}) for model R1 (2011 reference case) are given in Figure 6. No evidence of non-convergence from the trace statistics was found in the base or derived biomass parameters. Diagnostic plots suggested no evidence in non-convergence in the key parameters (B_0 and the selectivity parameters (see parameters 1–24 in Figure 7), but there was some evidence of lack of convergence in the median MCMC jump statistics for the annual shift parameters for the shelf catch-at-age proportions (see parameters 25–36 in Figure 7).

Convergence tests of Geweke (1992) and the Heidelberger & Welch (1983) stationarity and half-width tests passed all parameters, except that only some or all (depending on the test) of the annual shift parameters for the shelf fishery passed. However, sensitivity analyses of non-convergence in the annual shift parameters suggested that the effect of any non-convergence in these parameters on model conclusions were likely to be minimal (i.e., the choice of the annual selectivity parameters had little effect on resulting estimates of key biomass parameters within individual MCMC samples).

Autocorrelation lag plots (Figure 7) suggested that there was reasonable mixing in the MCMC chain with no evidence of autocorrelation. Diagnostics results for the other models showed similar results.

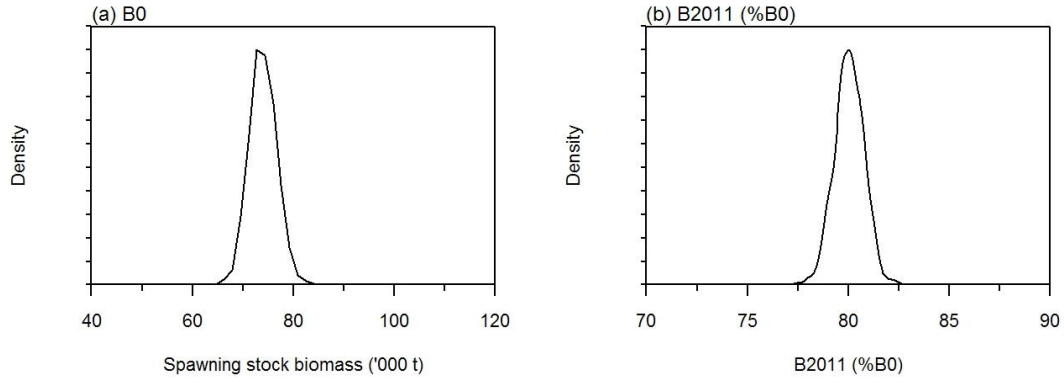

Figure 6: MCMC posterior distributions of (a) B_0 and (b) current biomass (%B_{2011}/B_0) for model R1 (2011 reference case).

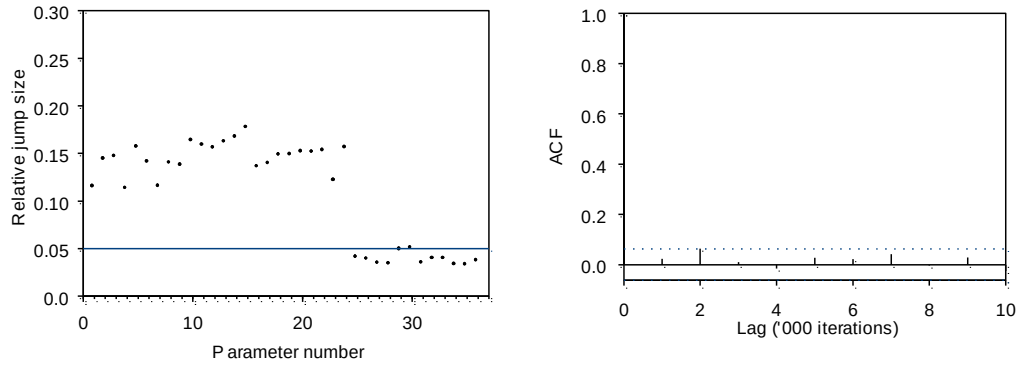

Figure 7: MCMC posterior diagnostic plots for model R1 (2011 reference case), showing (left) median relative jump size for all parameters (x-axis, labelled 1–24 for B_0 and selectivity parameters, 25–38 for shelf selectivity shift parameters), and (right) ACF lag plot for B_0.

3.4.2 MCMC estimates

Key output parameters for model runs R1, R2.3, and R3 are summarised in Table 12, and posterior estimates of the initial and current biomass for the 2011 reference case are given in Figure 8. MCMC estimates of initial (equilibrium) spawning stock abundance (B_0) for the 2011 reference case (model R1) were 73 870 t (95% credible intervals 69 070–78 880); current (B_{2011}) biomass was estimated as 80.0% B_0 (95% C.I.s 78.6–81.3).

For all models, the diagnostic plots of the observed proportions-at-age of the catch versus expected values did not indicate any strong evidence of inadequate model fit. The reference case model estimated depth shift values of 7.3 ykm^{-1} (5.5–9.2 ykm^{-1}) for the slope, and 2.4 ykm^{-1} (0.6–4.0 ykm^{-1}) for the north fishery. Estimated selectivity curves appeared reasonable, with strong evidence of domed shaped selectivity in all of the three fisheries (Figure 9). Estimated posterior densities of the observed and expected number of tags at length, by release event and recapture year, are given in Figure 10.

Table 12: Median MCMC estimates (and 95% credible intervals) of B_0, B_{2011}, and B_{2011} as $\%B_0$ for models R1–R3.

Model	B_0	B_{2011}	B_{2011} ($\%B_0$)
	62 080 (56 020–70 090)	–	–
R1	73 870 (69 070–78 880)	59 110 (54 370–64 240)	80.0 (78.6–81.3)
R2.3	74 460 (69 580–79 630)	57 800 (52 910–62 960)	77.6 (76.1–79.1)
R3	85 840 (80 220–91 700)	71 070 (65 440–77 070)	82.8 (81.6–83.9)

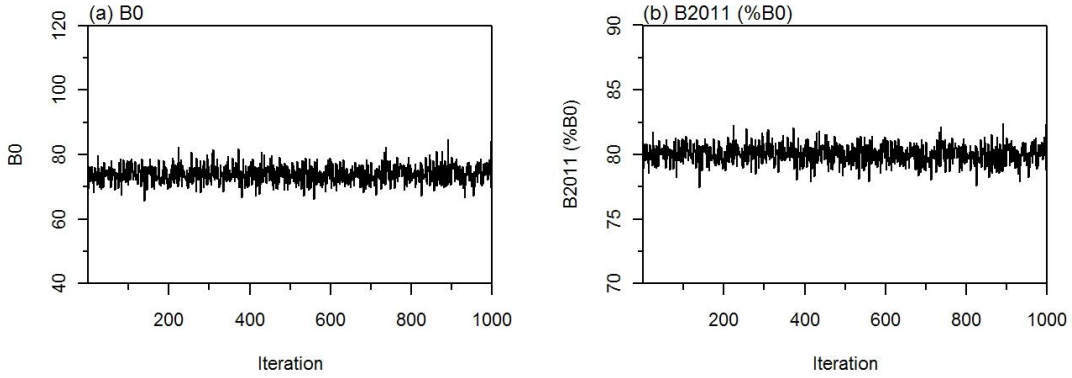

Figure 8: Posterior density estimates for (a) B_0 and (b) B_{2011} as a percent of B_0 for model R1 (2011 reference case).

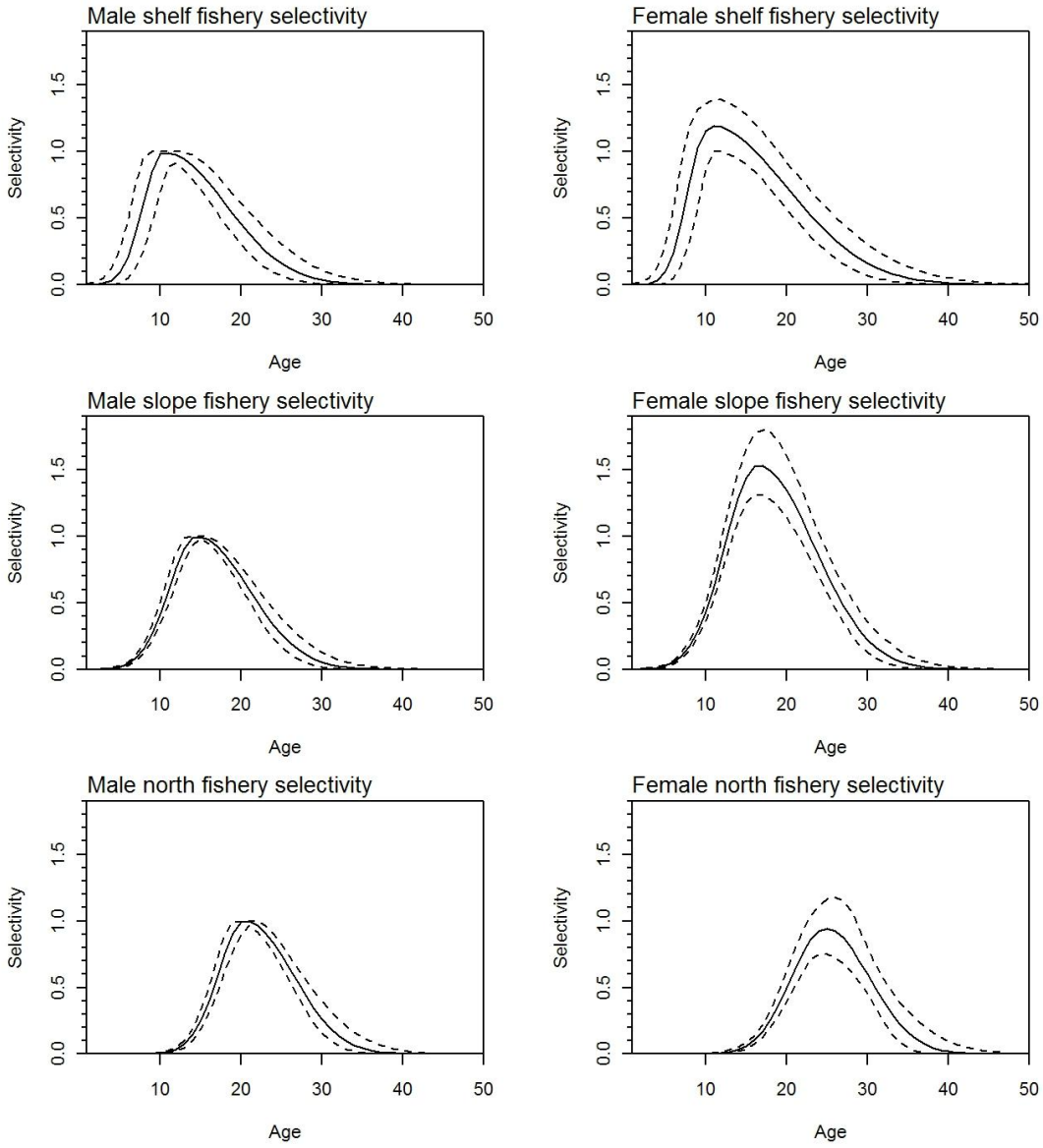

Figure 9: Estimated male and female selectivity ogives for the shelf, slope, and north fisheries for model R1 (2011 reference case). Solid lines indicate the median and dashed lines indicate the marginal 95% credible intervals.

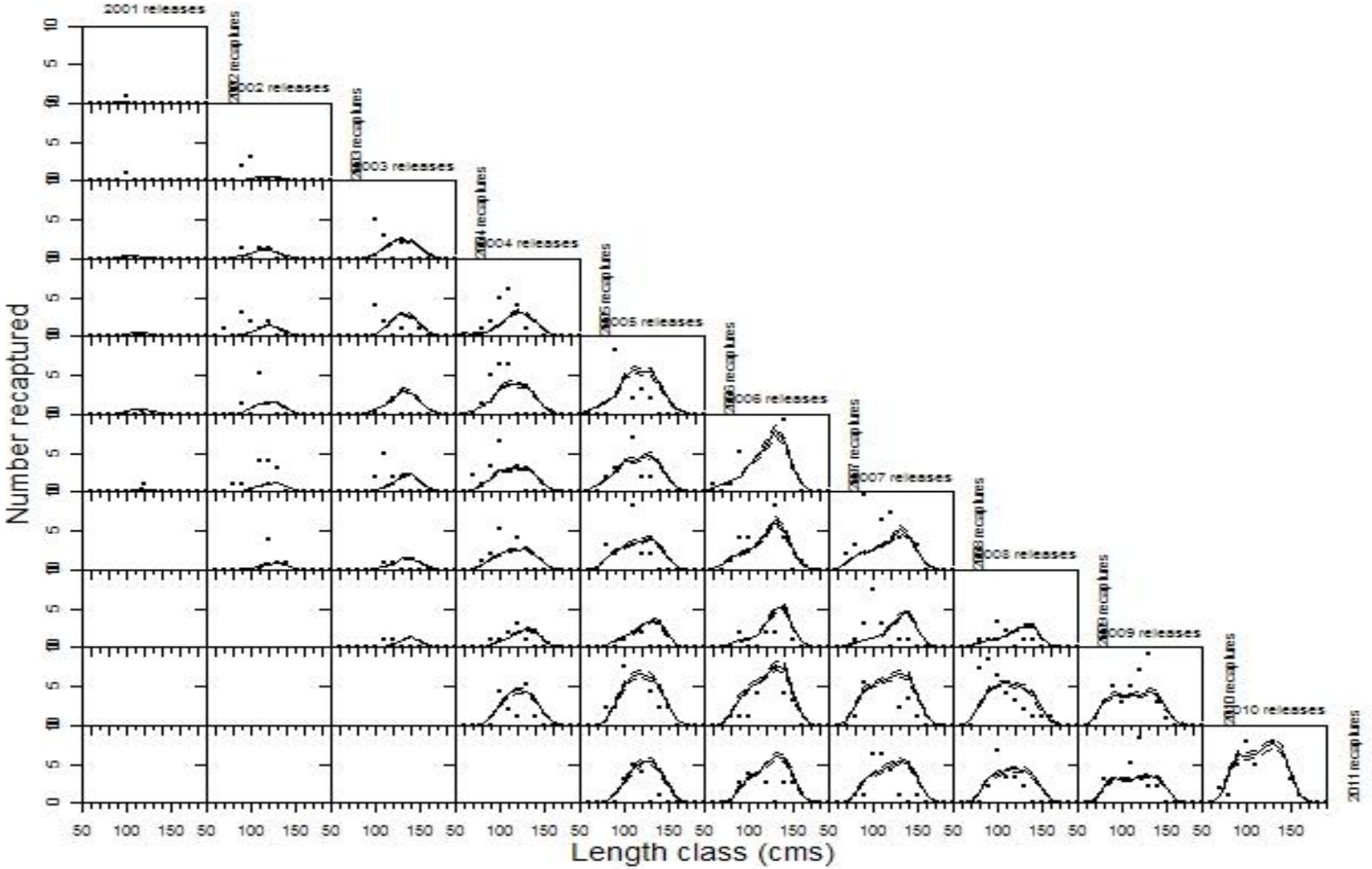

Figure 10: Model R1 (2011 reference case) observed (points) and posterior estimates (lines, MCMC median and 95% credible intervals) of the number of tags recaptured (y-axis) by length class (x-axis), year of release (columns), and year of recapture (rows).

3.5 Yield estimates

Yield estimates were based on an assumption of constant future catches, where the future catch was (i) set equal to the 2010 and 2011 catch limit (2850 t) and (ii) set equal to the catch that met the CCAMLR decision rules. The proportion of the catch from each area (shelf, slope, and north) was assumed to be equal to the mean annual proportion of fish taken from each of these areas for the years 2009–2011, i.e., 11.3%, 75.4%, and 13.3% respectively from the shelf, slope, and north areas.

Yields were calculated for model runs, R1, R2.3, and R3. For model R1 (2011 reference case), the decision rule risks of a constant catch at the 2009 catch limit (i.e., 2850 t) were calculated as $\max(Pr[SSB < 0.2 \times B_0]) = 0.0$ and $Pr[SSB_{+35} < 0.5 \times B_0] = 0.315$ (Table 13). Optimum yields (i.e., the maximum catch satisfying both $rule_1$ and $rule_2$) for model R1 were a constant future catch of 3282 t (Figure 11 and Table 13). For model R2.3 (including 90th percentile unaccounted mortality), the decision rule risks of a constant catch at the 2009 catch limit (i.e., 2850 t) were calculated as $\max(Pr[SSB < 0.2 \times B_0]) = 0.0$ and $Pr[SSB_{+35} < 0.5 \times B_0] = 0.316$ For model R3 (all vessel trips), the decision rule risks of a constant catch at the 2009 catch limit (i.e., 2850 t) were calculated as $\max(Pr[SSB < 0.2 \times B_0]) = 0.0$ and $Pr[SSB_{+35} < 0.5 \times B_0] = 0.145$

Table 13: CCAMLR decision rule risks ($rule_1$ and $rule_2$) under the 2009–2011 catch limit and the estimated CCAMLR yield (t).

Model		Catch limit = 2850 t		CCAMLR yield		
		$rule_1$	$rule_2$	Yield (t)	$rule_1$	$rule_2$
	2009 base case	0.002	0.500	–	–	–
R1	2011 reference case	0.000	0.315	3282	0.000	0.492
R2.3	90th percentile unaccounted mortality	0.000	0.316	3253	0.001	0.499
R3	All vessel trips	0.000	0.145	3810	0.001	0.500

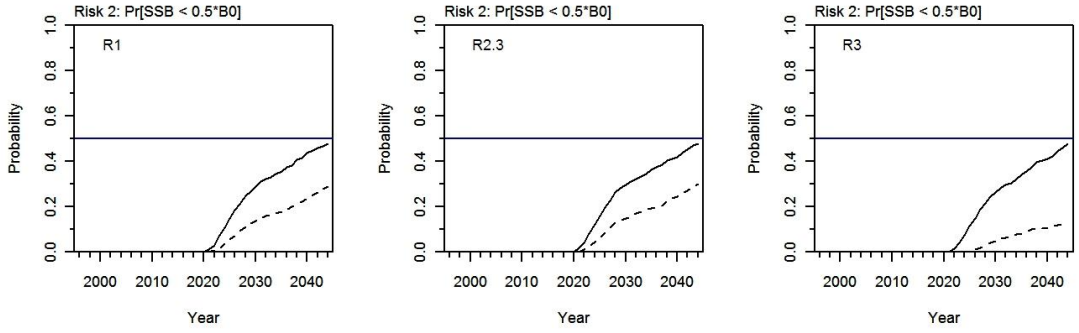

Figure 12: Estimated risks for models R1, R2.3 and R3 under the CCAMLR decision rules for (probability that SSB<0.5B_0 with the (dashed lines) current catch limit (2850 t) and (solid lines) maximum catch that meets the decision rule criteria for each model.

4. DISCUSSION

This paper presents assessment models for Antarctic toothfish (*Dissostichus mawsoni*) in the Ross Sea (Subareas 88.1 and SSRUs 88.2A–B), including data up to the end of the 2010–11 season. The reference model reported here was essentially an update of the 2009 base model assessment (Dunn & Hanchet 2009b), using the same model structure and similar sets of observations. The MCMC estimates of initial (equilibrium) spawning stock abundance (B_0) for the 2011 reference case (model R1) were 73 870 t (95% credible intervals 69 070–78 880); current (B_{2011}) biomass was estimated as 80.0% B_0 (95% C.I.s 78.6–81.3). The estimated yield for the 2011 reference case was 3282 t.

All of the models produced similar estimates of the decline in biomass due to fishing relative to initial conditions. However, scenarios R1 and R3 produced different estimates of initial biomass due to the alternative choice of tag data (i.e., selected trips versus all vessel trips respectively). The inclusion of the 90th percentile of unaccounted mortality had little effect on the estimates of initial biomass (R2.3). MCMC estimates of initial (equilibrium) spawning stock abundance (B_0) for models R2.3 and R3 were 74 460 (95% C.I.s 69 580–79 630) and 85 840 (95% C.I.s 80 220–91 700) respectively. As in 2009, the likelihood profiles indicated that the tag data provided the majority of the information on biomass to the model. Observations from different years of tag release and recapture had differing impacts on the model estimates. This is not unexpected because, as noted by Dunn & Hanchet (Dunn & Hanchet 2009b), the locations of the recaptures can be highly aggregated and most are seen to move only short distances. As with the 2009 assessment, this suggest that a key uncertainty underlying the current model is the effect of fish movement and spatial structure in the Antarctic toothfish population.

The 2011 reference case model estimates of initial and current biomass were higher than those estimated in 2009 base case. The application of the select algorithm in 2011 resulted in an increased proportion of vessel trips selected for the quality data set. Based on the retrospective analyses, the change appeared to be due to the selected vessel trips that were included by the algorithm interacting with the additional tag-recapture and release observations for 2010 and 2011. To some extent this change may be consistent with expectations, as there has been an increased emphasis on improved data quality in recent years. However, the sensitivity of the model to changes of this nature should be further investigated.

The effect of unaccounted fishing mortality arising from gear loss on model estimates of biomass and yield has not previously been discussed. The level of unaccounted mortality estimated by Webber & Parker (2011) is unlikely to have had any significant impact on the model estimates of biomass or yield, assuming a similar argument as for IUU catch (see Dunn & Hanchet 2006, Dunn & Hanchet 2007). However, we note that while the estimated yield from the model that included unaccounted mortality was similar to the yield from the 2011 reference case, these catch limits do not include provision for such additional mortality in the future.

5. ACKNOWLEDGMENTS

The authors would like to thank the scientific observers and fishing company staff who collected the data used for this analysis. We would also like to thank the members of the New Zealand Antarctic Fisheries Stock Assessment Working Group for helpful discussions and input into this paper. We thank David Ramm and Eric Appleyard for providing the data extracts from the CCAMLR Secretariat and assisting in the interpretation of the data. This project was funded by the New Zealand Ministry of Fisheries under project ANT2010/01.

6. REFERENCES

Agnew, D.J.; Clark, J.M.; McCarthy, P.A.; Unwin, M.; Ward, M.; Jones, L.; Breedt, G.; Plessis, S.D.; Heerdon, J.V.; Moreno, G. (2005). A study of Patagonian Toothfish (*Dissostichus eleginoides*) post-tagging survivorship in Subarea 48.3. WG-FSA-05/19. 11 p. CCAMLR. Unpublished report presented to the Fish Stock Assessment Working Group of CCAMLR

Bull, B.; Francis, R.I.C.C.; Dunn, A.; McKenzie, A.; Gilbert, D.J.; Smith, M.H.; Bian, R. (2008). CASAL (C++ algorithmic stock assessment laboratory): CASAL user manual v2.20-2008/02/14. *NIWA Technical Report 127*. 272 p.

Dunn, A.; Ballara, S.L.; Hanchet, S.M. (2007). An updated descriptive analysis of the toothfish (*Dissostichus spp.*) tagging programme in Subareas 88.1 & 88.2 up to 2006–07. WG-FSA-07/40. 25 p. CCAMLR. Unpublished manuscript presented to the Fish Stock Assessment Working Group of CCAMLR

Dunn, A.; Gilbert, D.J.; Hanchet, S.M. (2005a). Further development and progress towards evaluation of an Antarctic toothfish (*Dissostichus mawsoni*) stock model for the Ross Sea. WG-FSA-SAM-05/12. 24 p. CCAMLR. Unpublished manuscript presented to the Working Group on Statistics, Assessments, and Modelling of CCAMLR

Dunn, A.; Gilbert, D.J.; Hanchet, S.M. (2005b). A single-area stock assessment model of Antarctic toothfish (*Dissostichus mawsoni*) in the Ross Sea for the 2004–05 season. WG-FSA-05/33. 38 p. CCAMLR. Unpublished manuscript presented to the Fish Stock Assessment Working Group of CCAMLR

Dunn, A.; Gilbert, D.J.; Hanchet, S.M.; Bull, B. (2004). Development of an Antarctic toothfish (*Dissostichus mawsoni*) stock model for CCAMLR Subarea 88.1 for the years 1997–98 to 2003–04. WG-FSA-04/36. 39 p. CCAMLR. Unpublished manuscript presented to the Fish Stock Assessment Working Group of CCAMLR

Dunn, A.; Hanchet, S.M. (2006). Assessment models for Antarctic toothfish (*Dissostichus mawsoni*) in the Ross Sea including data from the 2005–06 season. WG-FSA-06/60. 26 p. CCAMLR. Unpublished manuscript presented to the Fish Stock Assessment Working Group of CCAMLR

Dunn, A.; Hanchet, S.M. (2007). Revised input parameters and implications for the Antarctic toothfish (*Dissostichus mawsoni*) stock assessment in Subareas 88.1 & 88.2. WG-SAM-07/06. 32 p. CCAMLR. Unpublished manuscript presented to the Working Group on Statistics, Assessments, and Modelling of CCAMLR

Dunn, A.; Hanchet, S.M. (2009a). Assessment models for Antarctic toothfish (*Dissostichus mawsoni*) in Subarea 88.2 SSRU E for the years 2002–03 to 2008–09. WG-FSA-09/41. 16 p. CCAMLR. Unpublished report presented at the Fish Stock Assessment Working Group of CCAMLR

Dunn, A.; Hanchet, S.M. (2009b). Assessment models for Antarctic toothfish (*Dissostichus mawsoni*) in the Ross Sea for the years 1997–98 to 2008–09. WG-FSA-09/40. 31 p. CCAMLR. Unpublished report presented at the Stock Assessment working Group of CCAMLR

Dunn, A.; Hanchet, S.M.; Devine, J. (2009a). Descriptive analysis of the toothfish (*Dissostichus* spp.) tagging program in Subareas 88.1 and 88.2 for the years 2000/01 to

2008/09. WG-FSA-09/38. 28 p. CCAMLR. Unpublished manuscript presented to the Fish Stock Assessment Working Group of CCAMLR

Dunn, A.; Hanchet, S.M.; Maxwell, K. (2005c). An updated descriptive analysis of the Antarctic toothfish (*Dissostichus mawsoni*) tagging scheme in the Ross Sea for the years 1997–98 to 2004–05. WG-FSA-05/34. 18 p. CCAMLR. Unpublished manuscript presented to the Fish Stock Assessment Working Group of CCAMLR

Dunn, A.; Horn, P.L.; Hanchet, S.M. (2006). Revised estimates of the biological parameters for Antarctic toothfish (*Dissostichus mawsoni*) in the Ross Sea. WG-FSA-SAM-06/08. 14 p. CCAMLR. Unpublished manuscript presented to the Working Group on Statistics, Assessments, and Modelling of CCAMLR

Dunn, A.; Rasmussen, S.; Hanchet, S.M. (2009b). Development of spatially explicit age-structured population dynamics operation models for Antarctic toothfish in the Ross Sea. WG-SAM-09/18. 44 p. CCAMLR. Unpublished manuscript presented to the Working Group on Statistics, Assessments, and Modelling of CCAMLR

Dunn, A.; Smith, M.H.; Agnew, D.J.; Mormede, S. (2011). Estimates of the tag loss rates for single and double tagged toothfish (*Dissostichus mawsoni*) fishery in the Ross Sea. CCAMLR-WG-SAM-11/18. 13 p. CCAMLR. Unpublished report presented at the Stock Assessment Methods working group of CCAMLR

Gelman, A.B.; Carlin, J.S.; Stern, H.S.; Rubin, D.B. (1995). Bayesian data analysis. Chapman and Hall, London. 526 p.

Geweke, J. (1992). Evaluating the accuracy of sampling-based approaches to calculating posterior moments. *In*: Bayesian Statistics, 4. Bernardo, J.M.; Berger, J.O.; Dawid, A.P.; Smith, A.F.M. (eds.). Clarendon Press, Oxford. pp 169–194.

Gilks, W.R.; Richardson, S.; Spiegelhalter, D.J. (eds.) (1998). Markov chain Monte Carlo in practice. *Interdisciplinary statistics*. 399 p. Chapman and Hall/CRC Press, Boca Raton, Florida.

Hanchet, S.M.; Stevenson, M.L.; Phillips, N.L.; Dunn, A. (2005). A characterisation of the toothfish fishery in Subareas 88.1 and 88.2 from 1997–98 to 2004–05. WG-FSA-05/29. 27 p. CCAMLR. Unpublished report presented to the Fish Stock Assessment Working Group of CCAMLR

Heidelberger, P.; Welch, P. (1983). Simulation run length control in the presence of an initial transient. *Operations Research 31*: 1109–1144.

Middleton, D.A.J. (2009). The selection of trips based on data metrics for the assessment of Antarctic toothfish in the Ross Sea. WG-FSA-09/35. 10 p. CCAMLR. Unpublished report presented at the Fish Stock Assessment working group of CCAMLR

Mormede, S.; Dunn, A.; Hanchet, S.M. (2011a). Descriptive analysis of the toothfish (*Dissostichus* spp.) tagging programme in Subareas 88.1 & 88.2 for the years 2000-01 to 2010-11. WG-FSA-11/xx. CCAMLR. Unpublished report presented at the Fish Stock Assessment working group of CCAMLR

Mormede, S.; Dunn, A.; Pinkerton, M. (2011b). Generic modelling tools for the assessment of marine populations. *In*: The Kerguelen Plateau: Marine ecosystem and Fisheries. Duhamel, G.; Welsford, D. (eds.). Cybium, Paris. pp 257-262.

Parker, S.; Grimes, P.J. (2009). Length and age at spawning of Antarctic toothfish *Dissostichus mawsoni* in the Ross Sea. WG-FSA-09/7. 18 p. CCAMLR. Unpublished manuscript presented to the Fish Stock Assessment Working Group of CCAMLR

Phillips, N.L.; Dunn, A.; Hanchet, S.M. (2005). Stratification of catch-at-length data using tree based regression. An example using Antarctic toothfish (*Dissostichus mawsoni*) in the Ross Sea. WG-FSA-SAM-05/8. 15 p. CCAMLR. Unpublished report presented to the Stock Assessment Methods Subgroup of the Fish Stock Assessment Working Group of CCAMLR

SC-CAMLR-XXIII (2004). Report of the twenty-third meeting of the scientific committee. CCAMLR, Hobart, Australia. 25–29 October 2004.

SC-CAMLR-XXIX (2011). Report of the twenty ninth meeting of the scientific committee. CCAMLR

SC-CAMLR-XXVIII (2009). Report of the twenty-eighth meeting of the Scientific Committee. CCAMLR, Hobart, Australia. 584 p. CCAMLR.

Smith, B.J. (2003). Bayesian output analysis program (BOA). Version 1.0 user's manual. Unpublished manuscript. 45 p. University of Iowa College of Public Health. (*see* http://www.public-health.uiowa.edu/boa)

Stevenson, M.J.; Hanchet, S.M.; Mormede, S.; Dunn, A. (2011). A characterisation of the toothfish fishery in Subareas 88.1 and 88.2 from 1997-98 to 2010-11. WG-FSA-11/xx. CCAMLR. Unpublished report presented at the Fish Stock Assessment working group of CCAMLR

Webber, D.N.; Parker, S.J. (2011). Gear loss and unaccounted fishing mortality in the Ross Sea longline fishery. WG-FSA-11/xx. CCAMLR. Unpublished report presented at the Fish Stock Assessment working group of CCAMLR

WG-FSA-SAM (2006). Report of the WG-FSA Subgroup on Assessment Methods (Walvis Bay, Namibia, 10 to 14 July 2006). WG-FSA-06/6. 66 p

APPENDIX A: MPD MODEL FITS

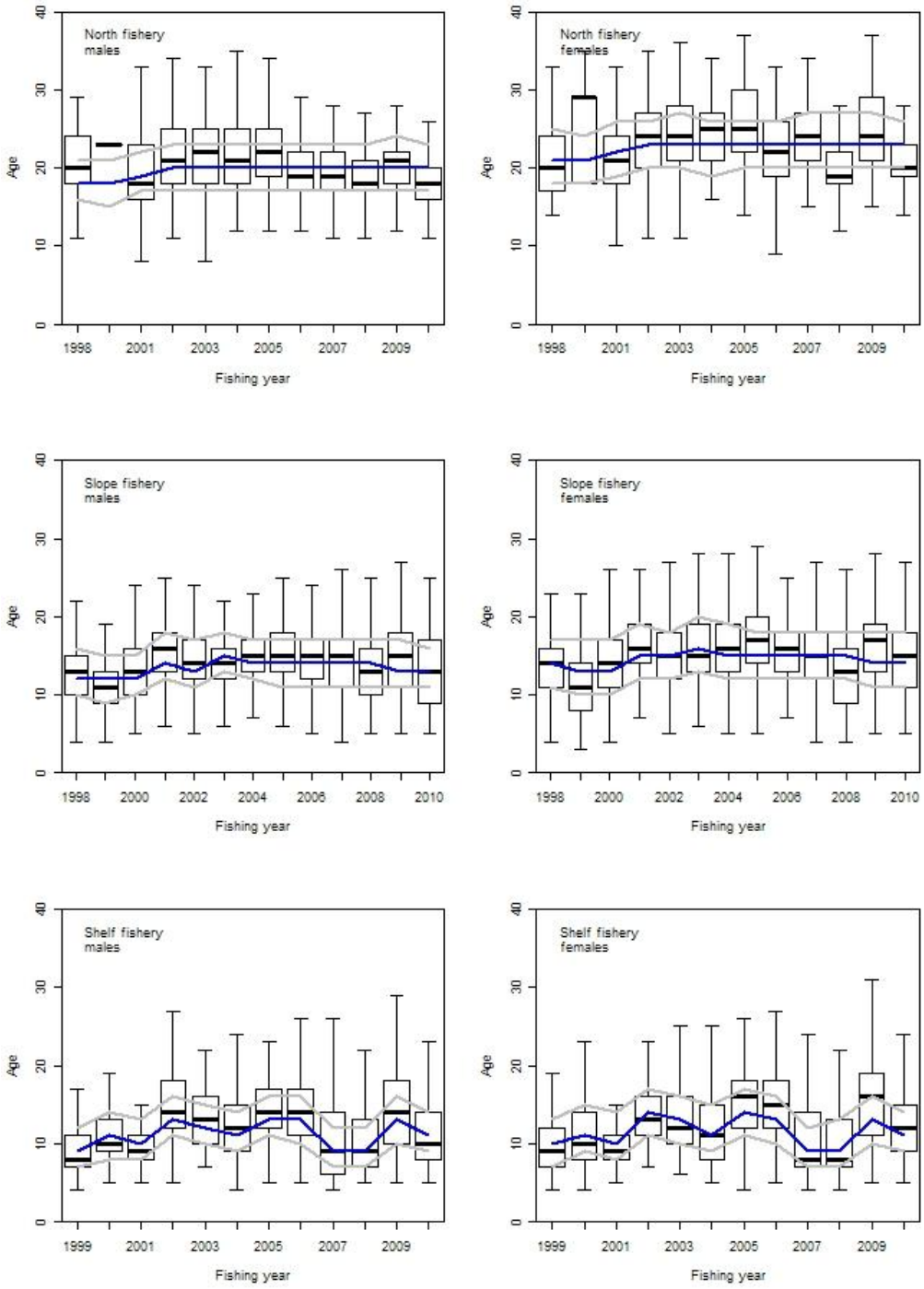

Figure A1: Observed boxplot of yearly ages by sex for the north, shelf, and slope fisheries, and mean (blue line), and quartiles (heavy grey lines) expected ages from the model. The whiskers of the boxplot represent the maximum range.

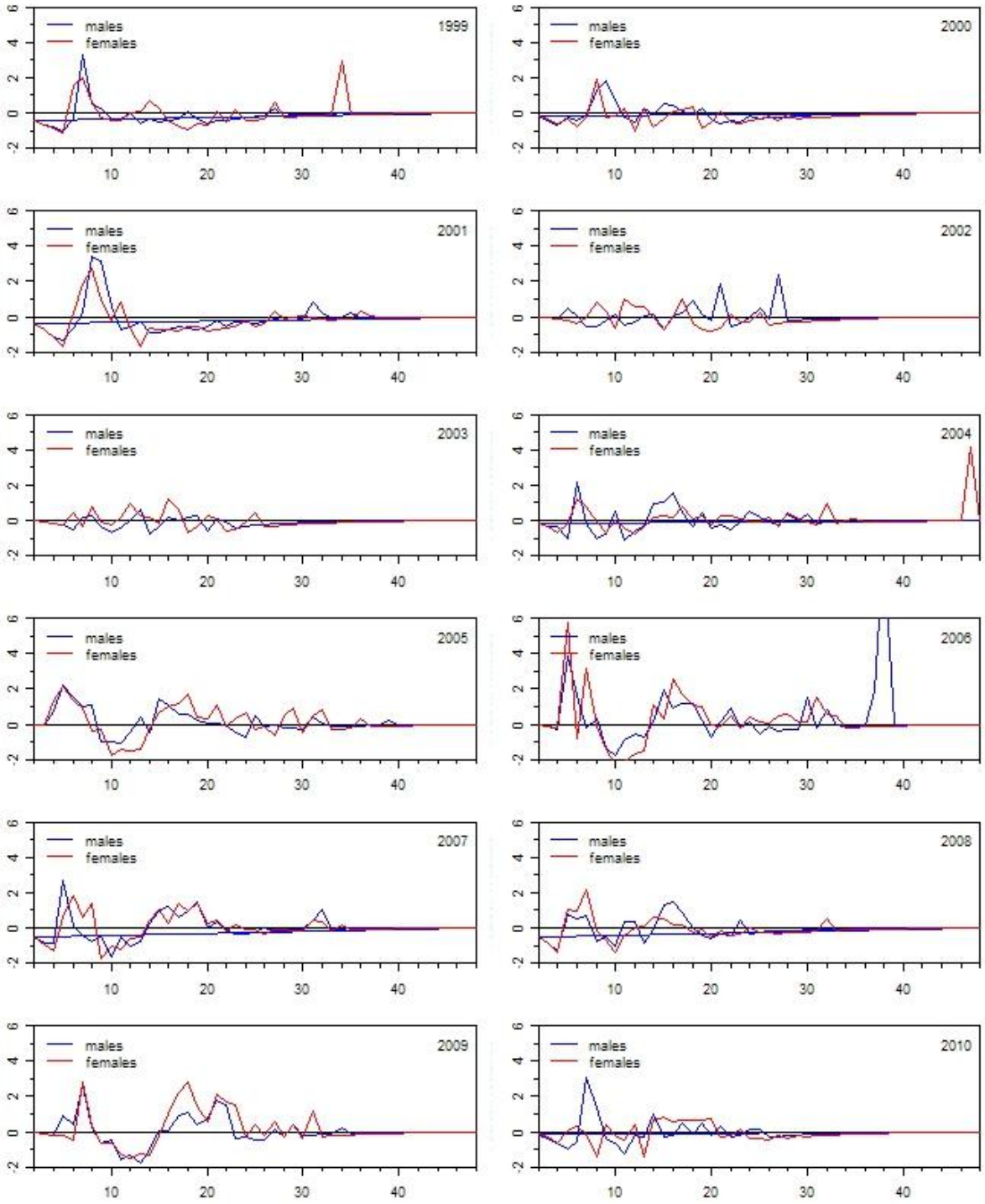

Figure A2: Pearson residuals of the age frequency as a function of age for the shelf fishery for individual years and all years combined. Males (blue) and females (red) are plotted separately. Boxplots represent median, interquartile, and maximum range.

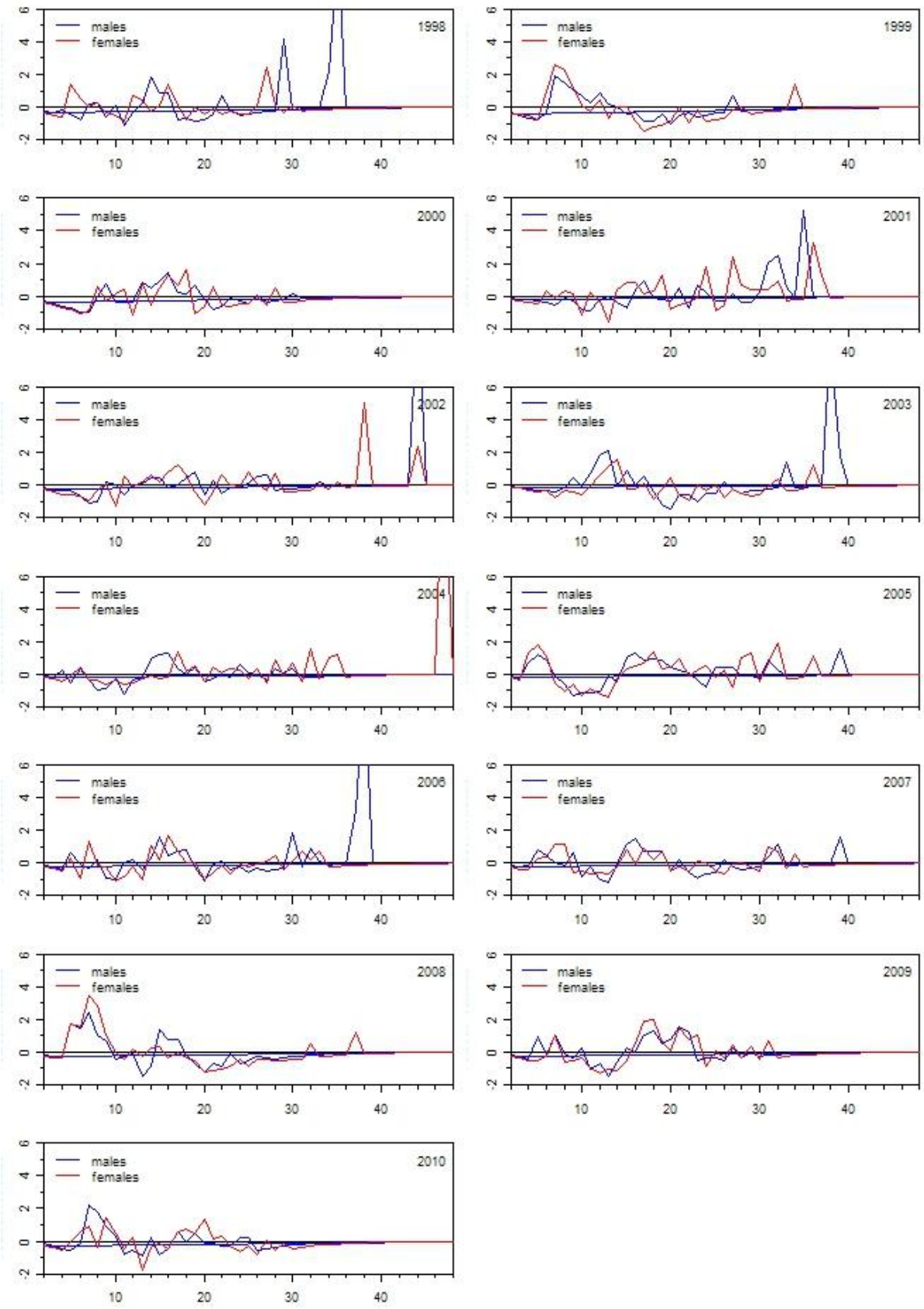

Figure A3: Pearson residuals of the age frequency as a function of age for the slope fishery for individual years and all years combined. Males (blue) and females (red) are plotted separately. Boxplots represent median, interquartile, and maximum range.

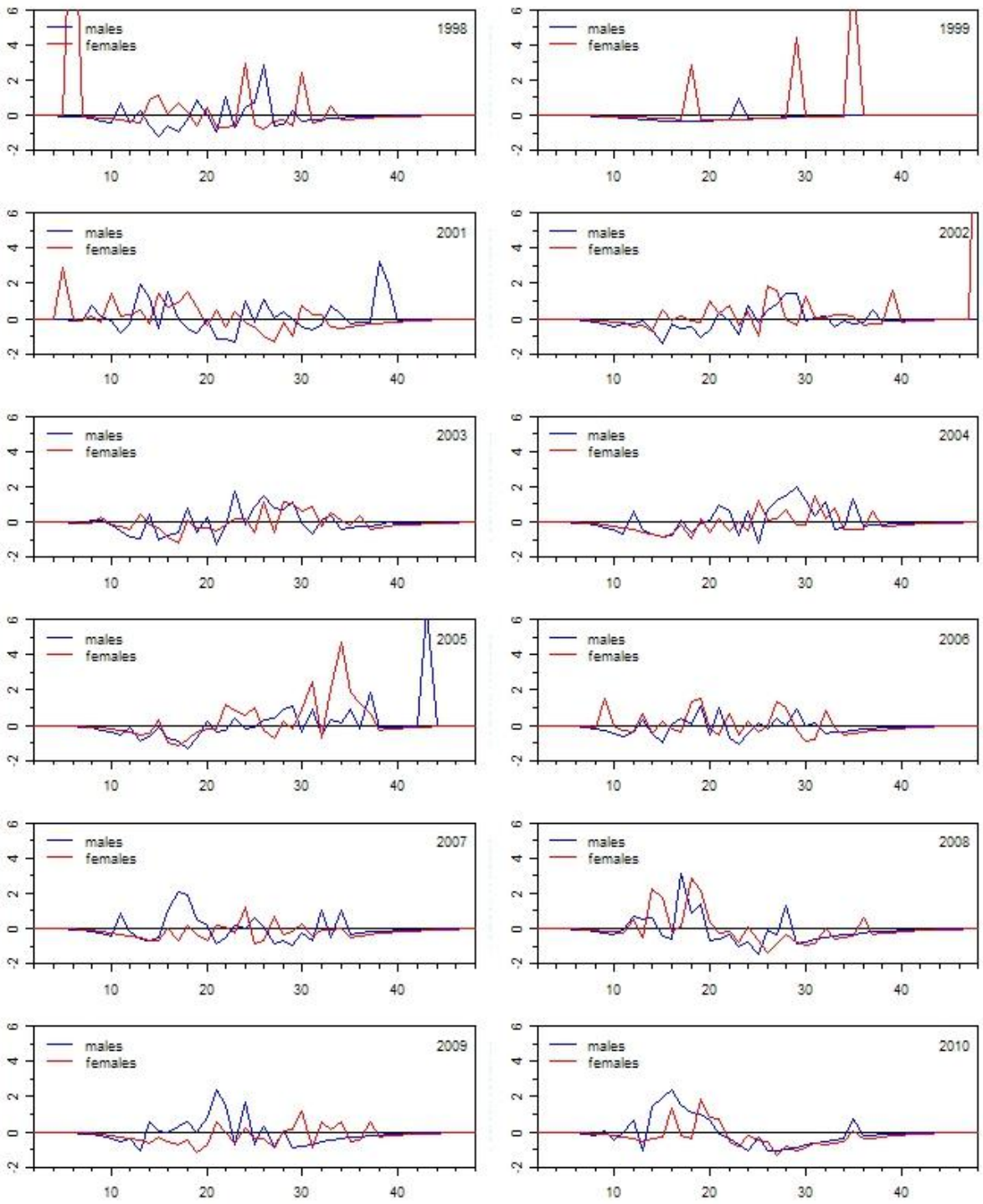

Figure A4: Pearson residuals of the age frequency as a function of age for the north fishery for individual years and all years combined. Males (blue) and females (red) are plotted separately. Boxplots represent median, interquartile, and maximum range.

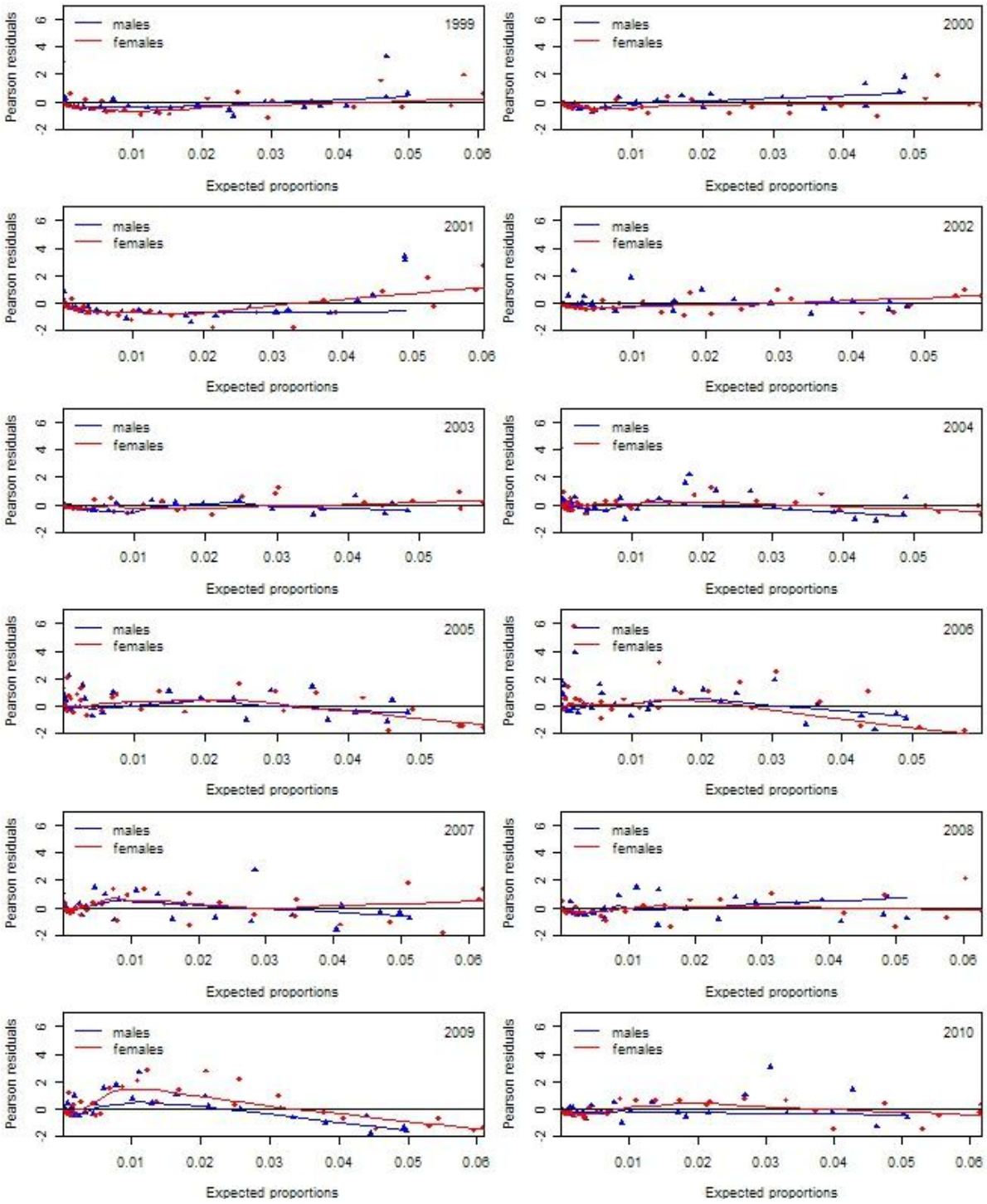

Figure A5: Pearson residuals of the age frequency as a function of proportions of fish for the shelf fishery for each year and distribution for all years combined. Males (blue squares) and females (pink circles), and lowess curve.

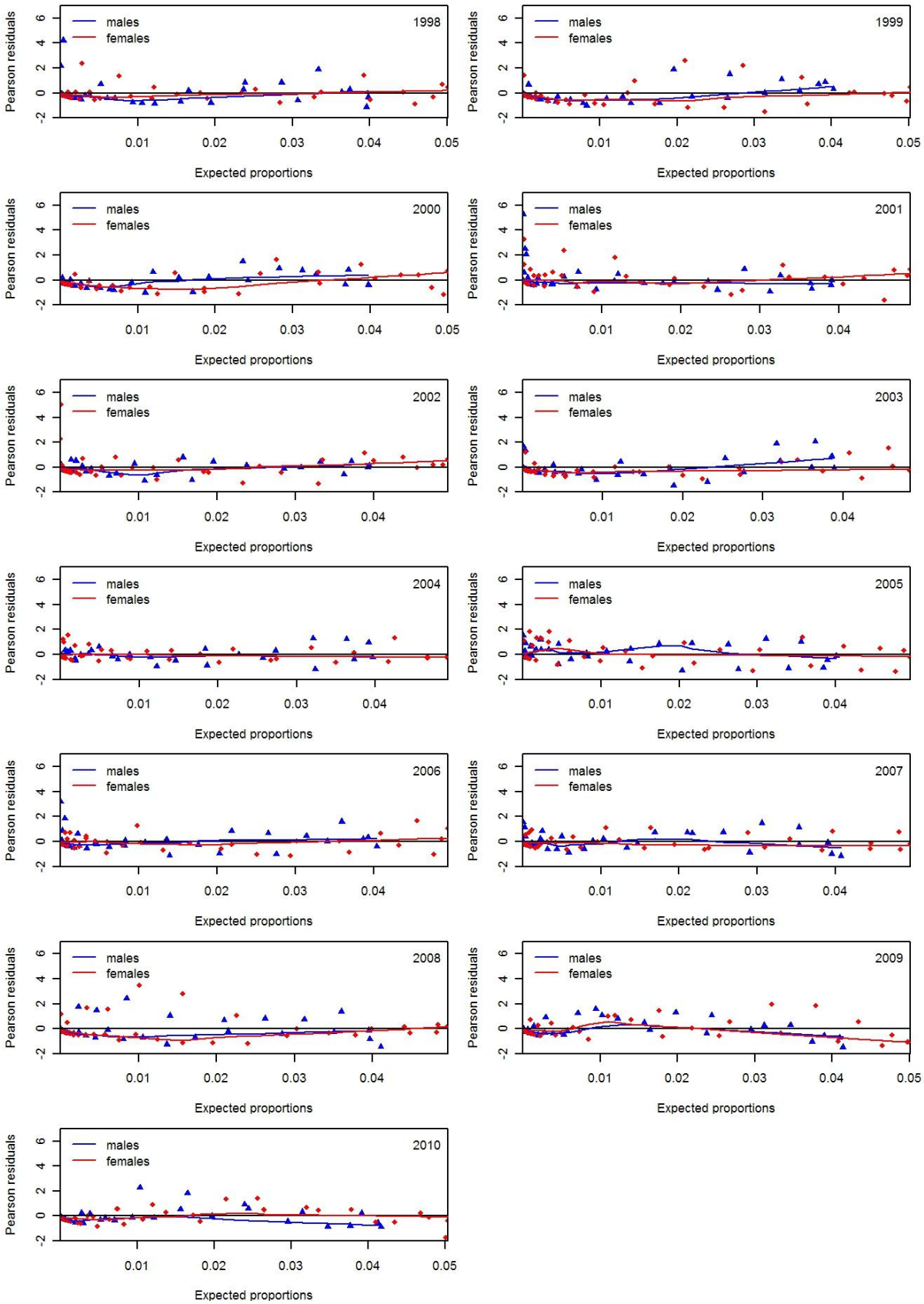

Figure A5: Pearson residuals of the age frequency as a function of proportions of fish for the north fishery for each year and distribution for all years combined. Males (blue squares) and females (pink circles), and lowess curve.

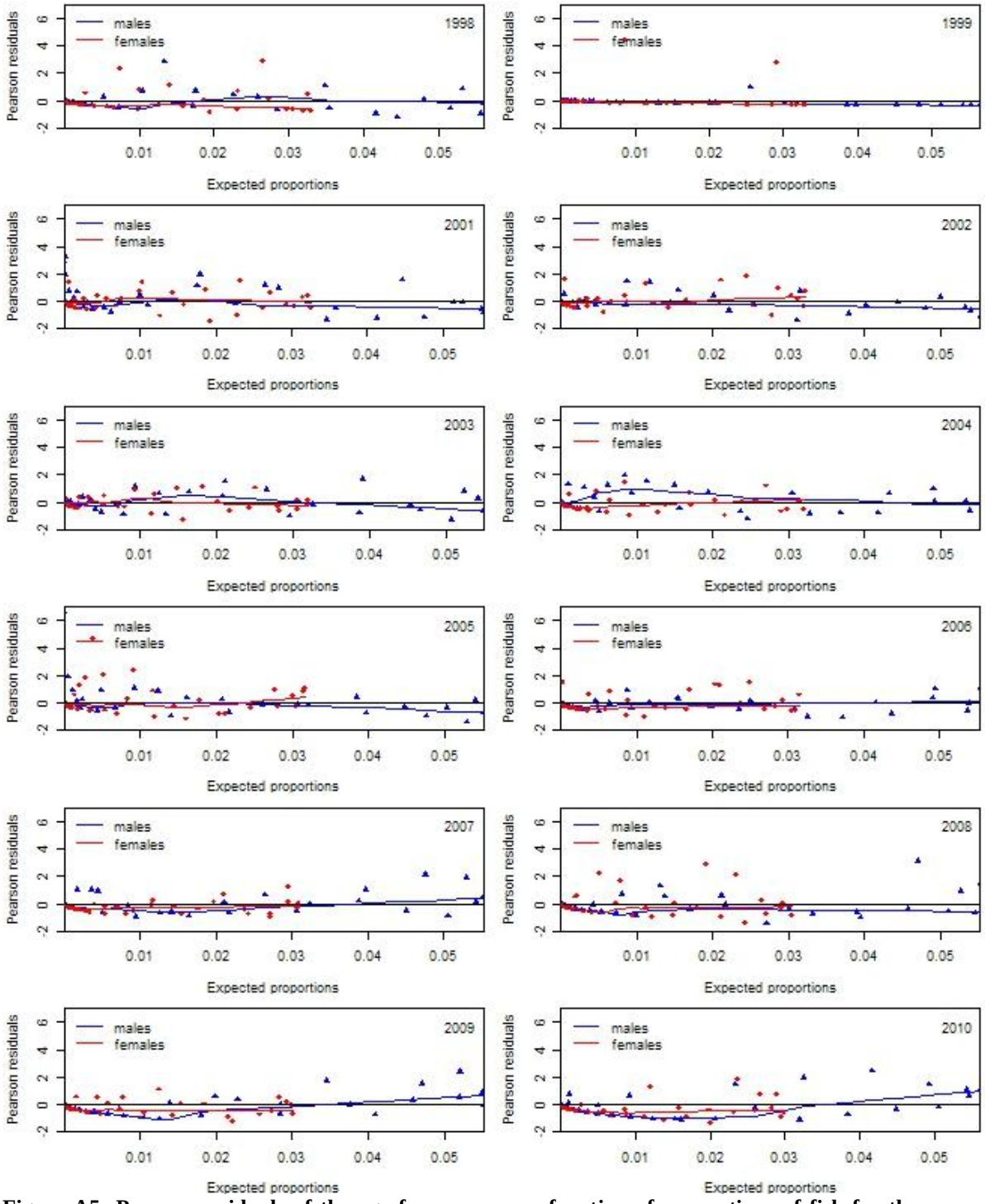

Figure A5: Pearson residuals of the age frequency as a function of proportions of fish for the north fishery for each year and distribution for all years combined. Males (blue squares) and females (pink circles), and lowess curve.

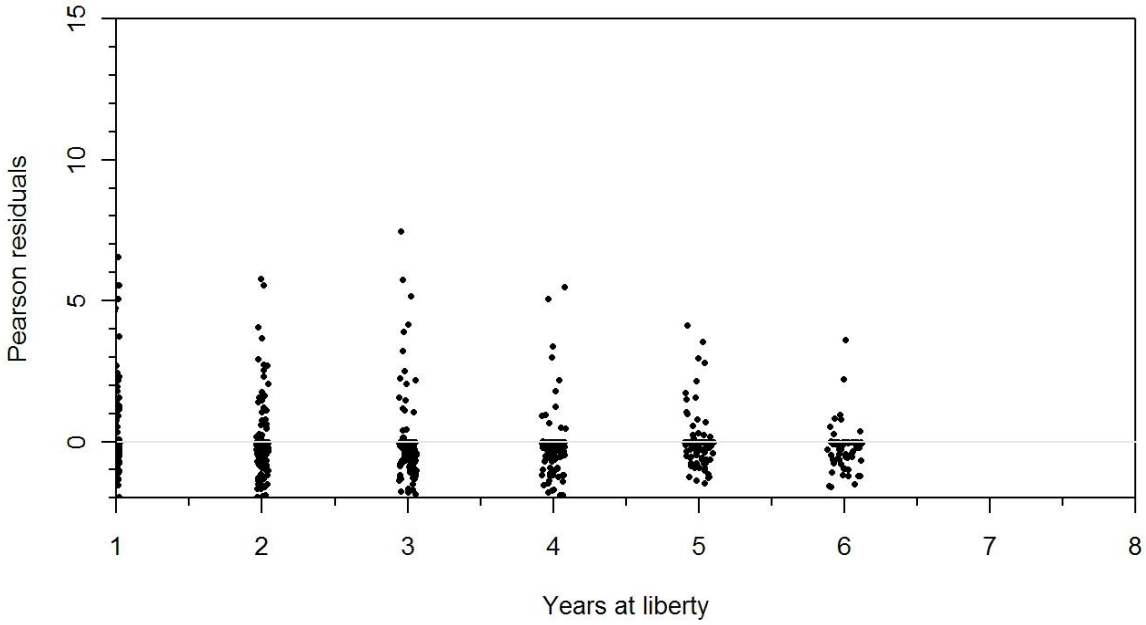

Figure A15: Observed Pearson residuals of the tag recapture fits as a function of years at liberty

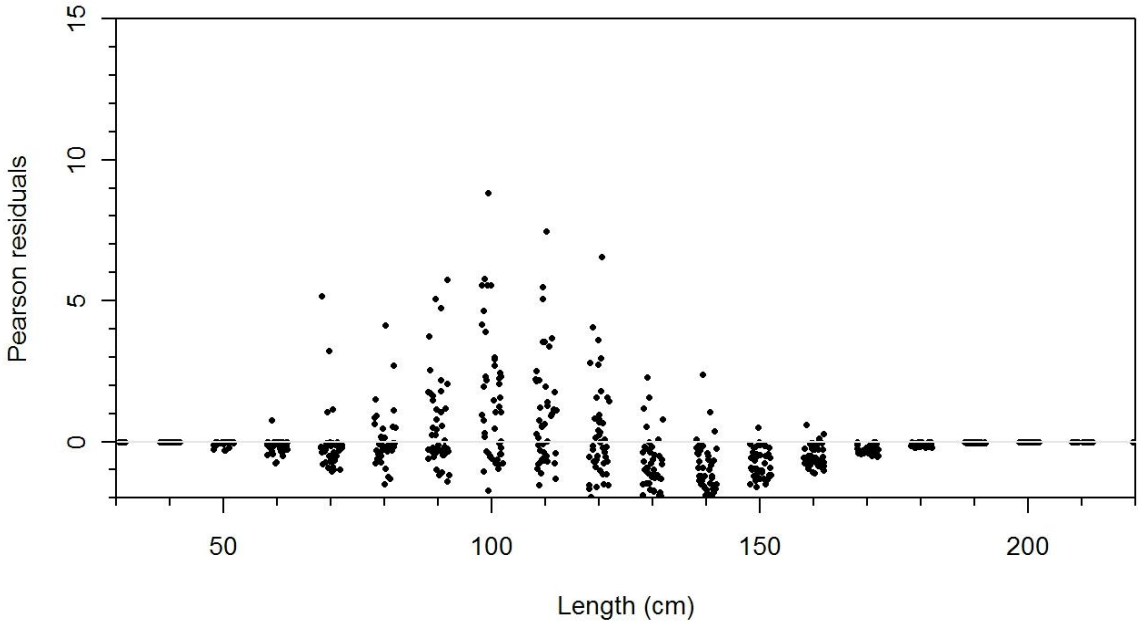

Figure A15: Observed Pearson residuals of the tag recapture fits as a function of length.

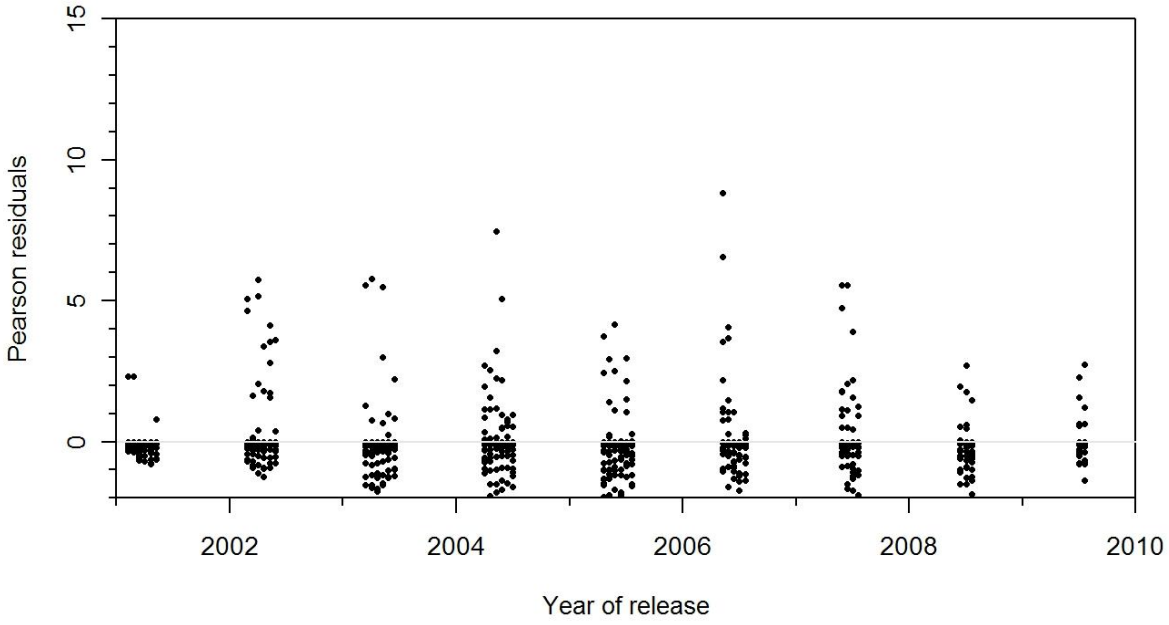

Figure A18: Observed Pearson residuals of the tag recapture fits as a function of the year of release. The x-axis is jittered by the year of release.

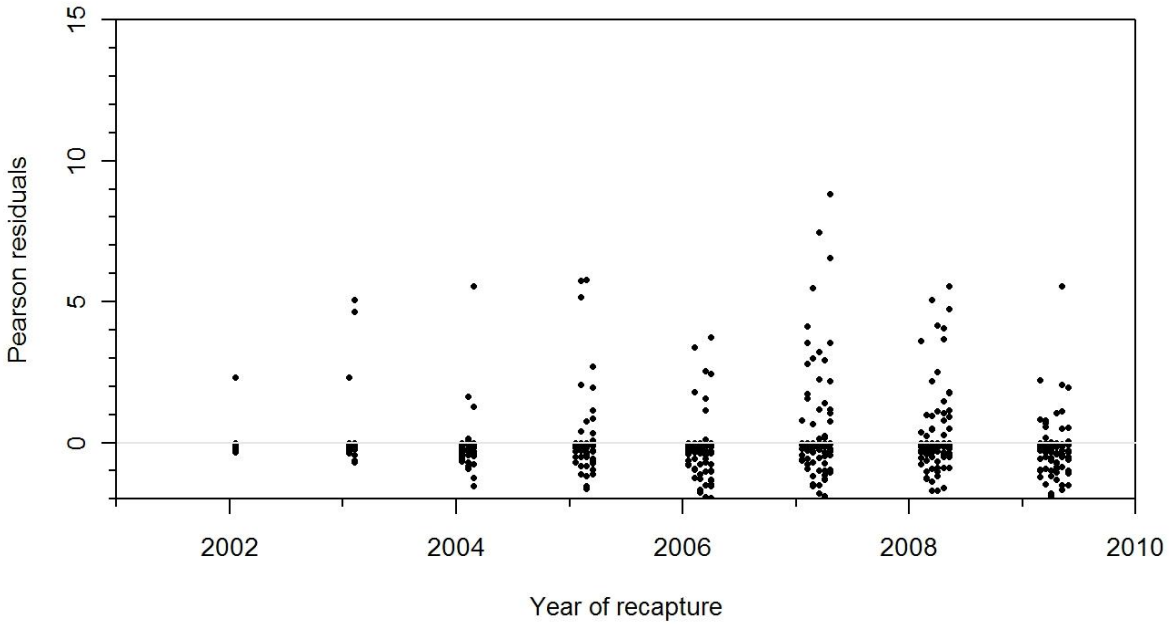

Figure A18: Observed Pearson residuals of the tag recapture fits as a function of the year of recapture. The x-axis is jittered by the year of recapture.

APPENDIX B: MCMC FITS AND TRACES

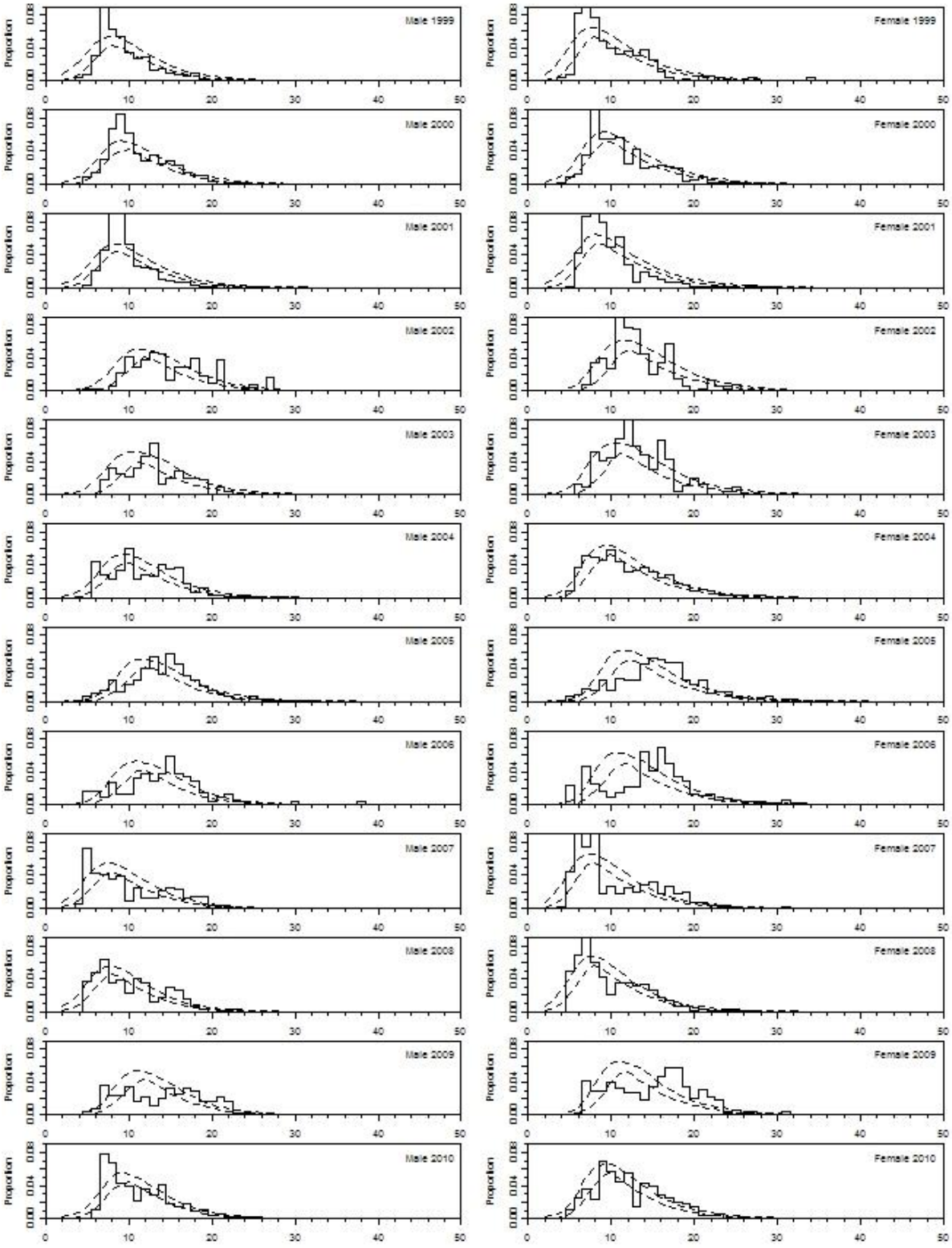

Figure B1: 90% credible interval of MCMC predicted (dashed) and observed proportions (y-axis) at age (x-axis) in the catch for the shelf fishery, model R1 (2011 reference case).

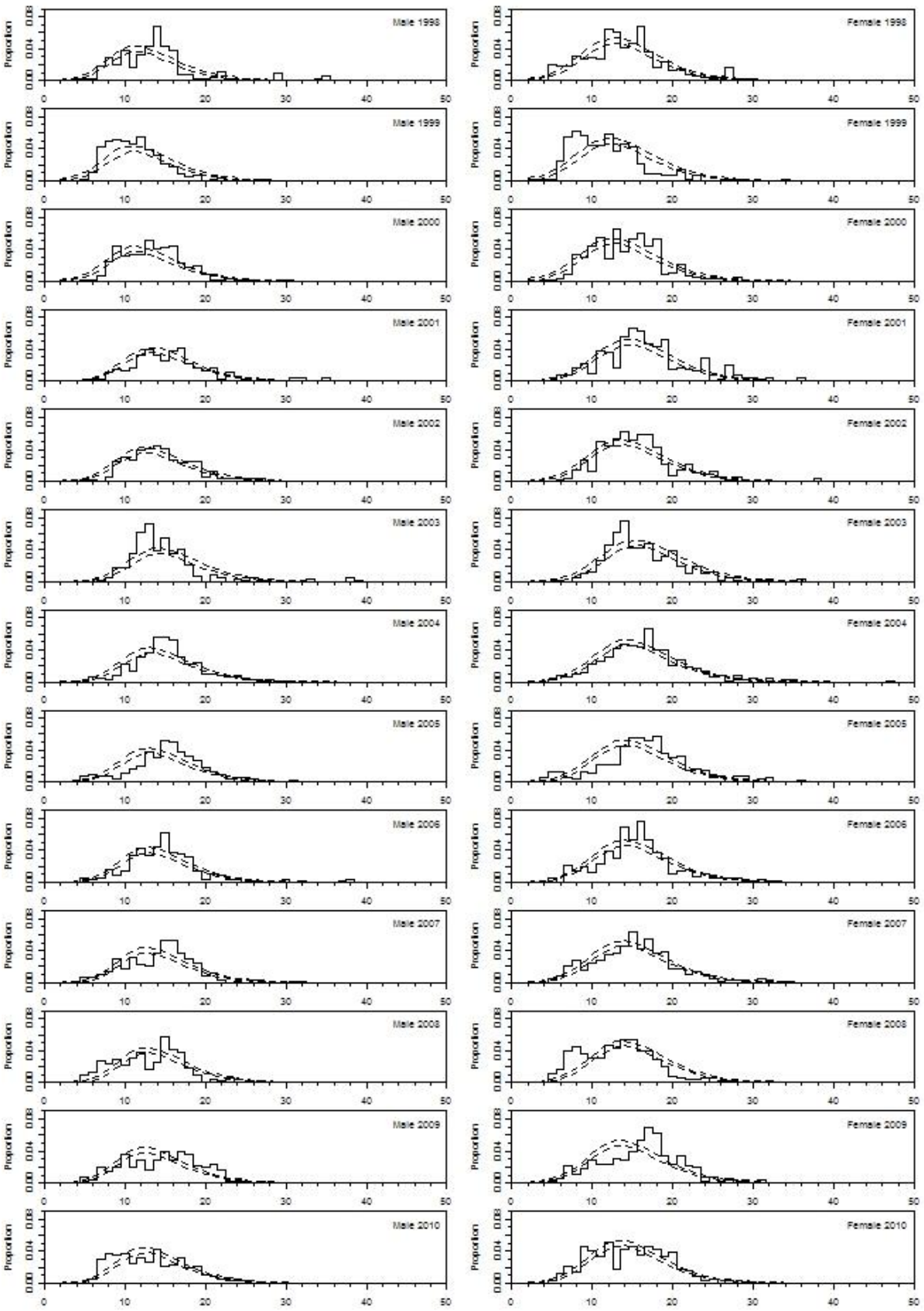

Figure B2: 90% credible interval of MCMC predicted (dashed) and observed proportions (y-axis) at age (x-axis) in the catch for the slope fishery, model R1 (2011 reference case).

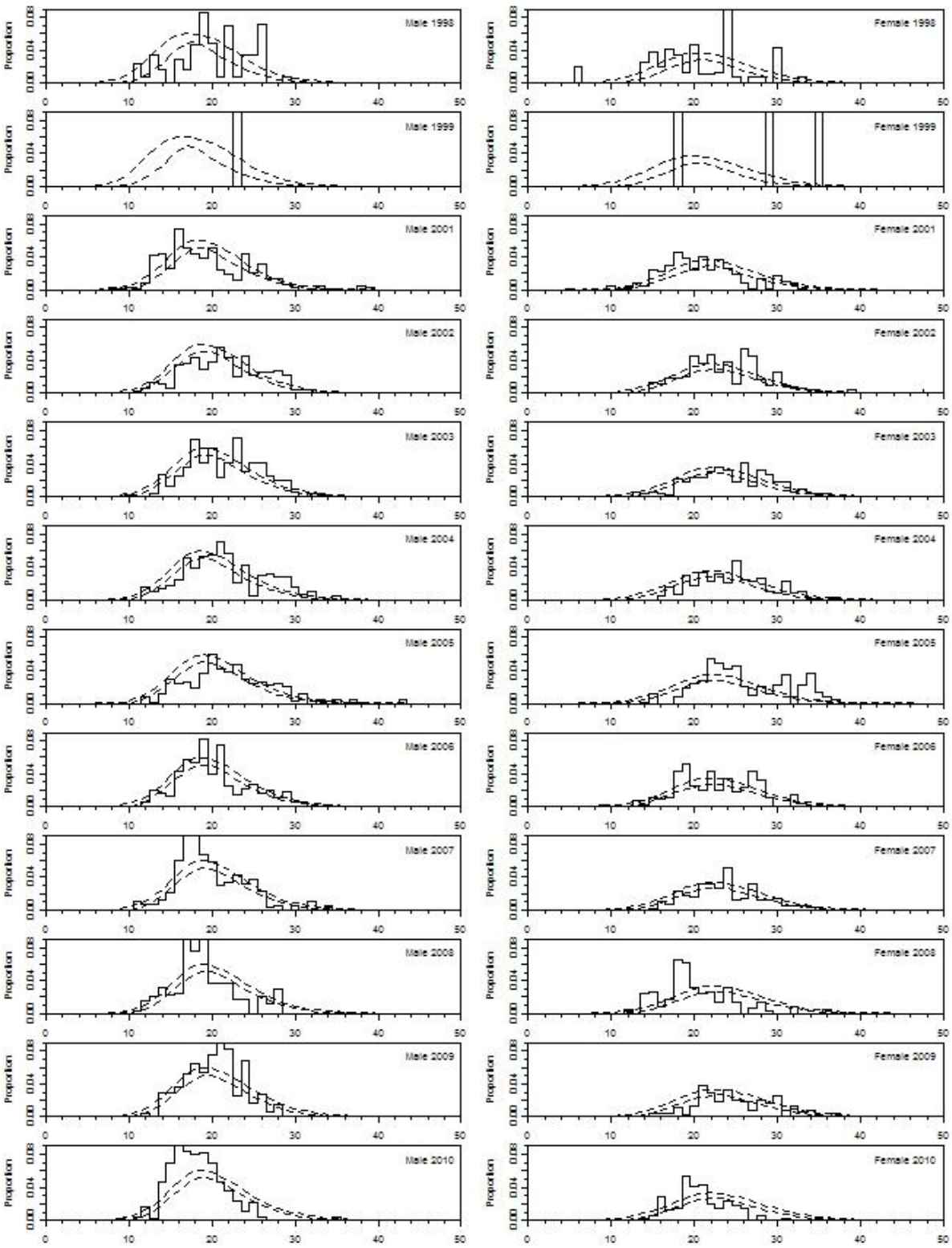

Figure B3: 90% credible interval of MCMC predicted (dashed) and observed proportions (y-axis) at age (x-axis) in the catch for the north fishery, model R1 (2011 reference case).

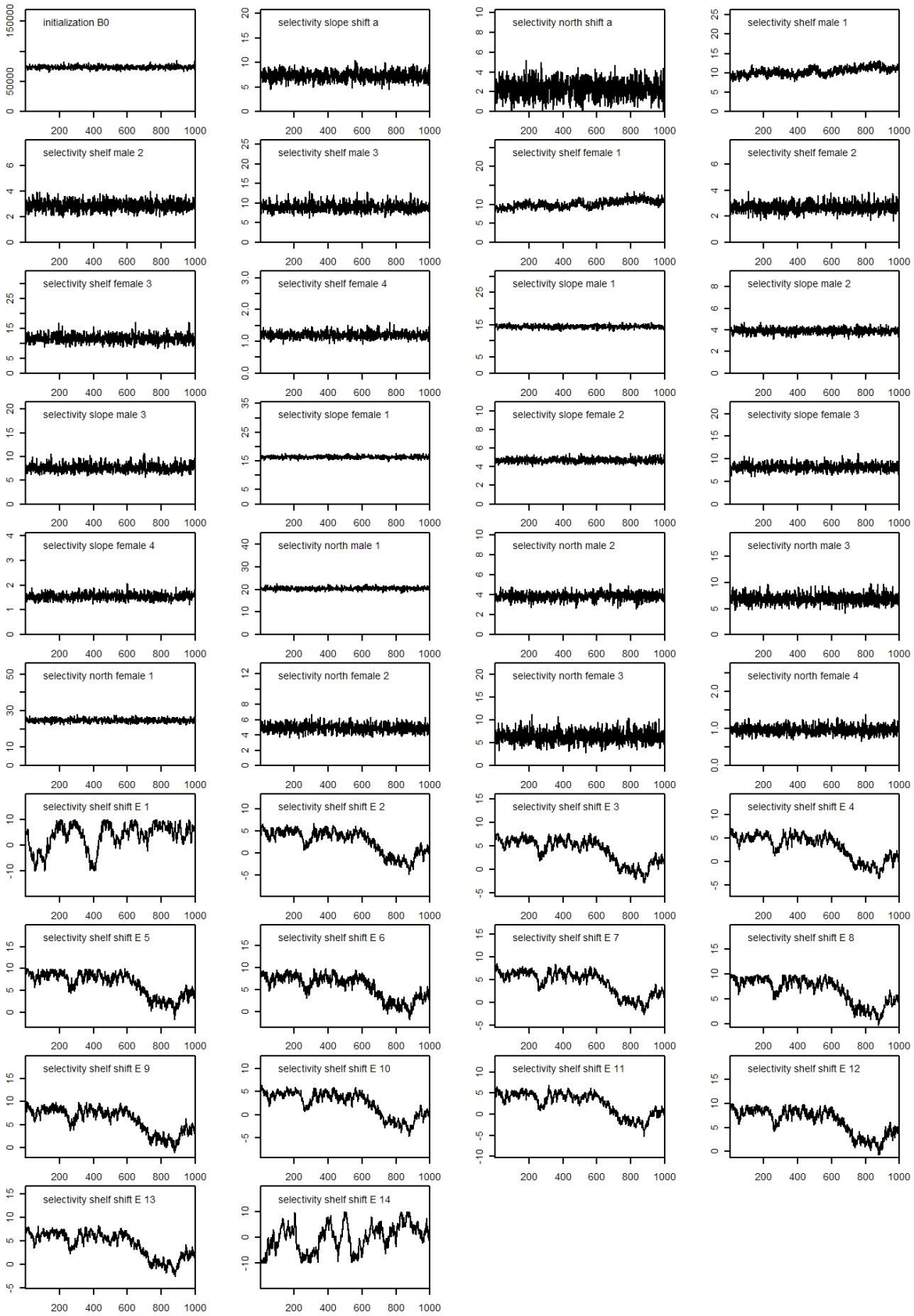

Figure B4: MCMC trace of all estimable parameters for model R1 (2011 reference case).